



Original article

Multifunctional tacrine–flavonoid hybrids with cholinergic, β -amyloid-reducing, and metal chelating properties for the treatment of Alzheimer's disease



Su-Yi Li ^a, Xiao-Bing Wang ^a, Sai-Sai Xie ^a, Neng Jiang ^a, Kelvin D.G. Wang ^a, He-Quan Yao ^b, Hong-Bin Sun ^b, Ling-Yi Kong ^{a,*}

^a State Key Laboratory of Natural Medicines, Department of Natural Medicinal Chemistry, China Pharmaceutical University, 24 Tong Jia Xiang, Nanjing 210009, People's Republic of China

^b Center for Drug Discovery, College of Pharmacy, China Pharmaceutical University, 24 Tong Jia Xiang, Nanjing 210009, People's Republic of China

ARTICLE INFO

Article history:

Received 26 April 2013

Received in revised form

5 September 2013

Accepted 8 September 2013

Available online 21 September 2013

Keywords:

Alzheimer's disease

Flavonoid

Tacrine

Cholinesterase

β -Amyloid aggregation

Metal chelator

ABSTRACT

A new series of tacrine–flavonoid hybrids (**13a–u**) had been designed, synthesized, and evaluated as multifunctional cholinesterase (ChE) inhibitors against Alzheimer's disease (AD). In vitro studies showed that most of the molecules exhibited a significant ability to inhibit ChE and self-induced amyloid- β ($A\beta_{1-42}$) aggregation. Kinetic and molecular modeling studies also indicated compounds were mixed-type inhibitors, binding simultaneously to active, peripheral and mid-gorge sites of AChE. Particularly, compound **13k** was found to be highly potent and showed a balanced inhibitory profile against ChE and self-induced $A\beta_{1-42}$ aggregation. Moreover, it also showed excellent metal chelating property and low cell toxicity. These results suggested that **13k** might be an excellent multifunctional agent for AD treatment.

© 2013 Elsevier Masson SAS. All rights reserved.

1. Introduction

Alzheimer's disease (AD), the most common form of adult onset dementia, is a complex neurodegenerative process occurring in the central nervous system (CNS), characterized by progressive cognitive decline and memory loss [1,2]. Although the etiology of AD is not fully known at present, several factors are considered to play significant roles in the pathophysiology of AD. These include the deposits of aberrant proteins namely β -amyloid ($A\beta$) and τ -protein, oxidative stress, dyshomeostasis of biometals, and low levels of acetylcholine (ACh) [3,4].

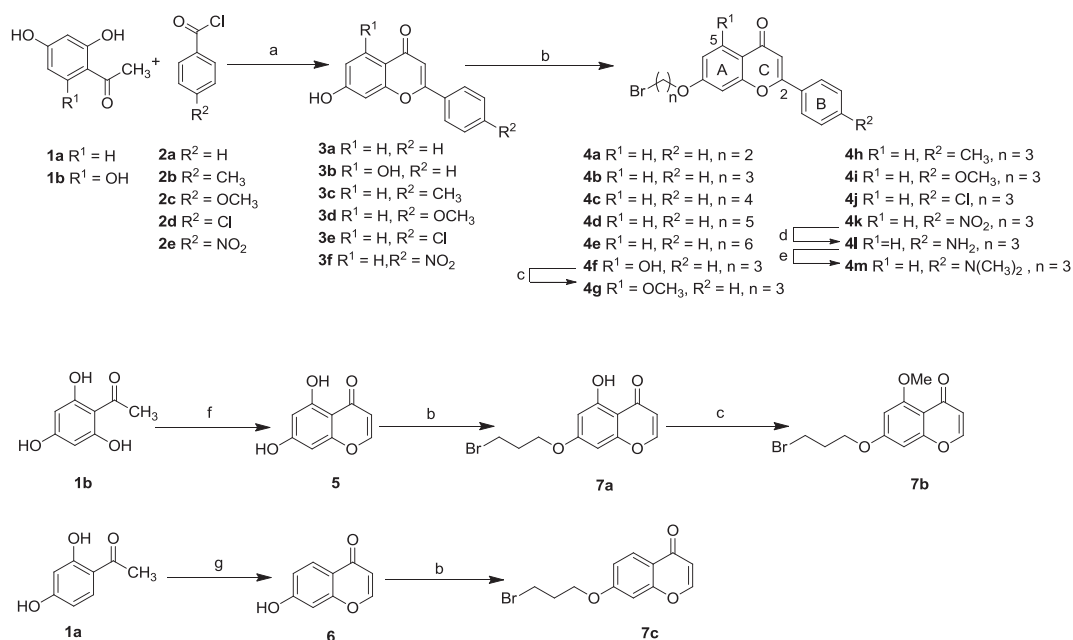
Current clinical therapy for AD patients is mainly based on the cholinergic hypothesis [5,6]. It suggests that, the decline of ACh level leads to cognitive and memory deficits, and sustaining or recovering the cholinergic function is supposed to be clinically beneficial. ACh can be degraded by two types of cholinesterases, namely AChE and butyrylcholinesterase (BuChE) [7]. The

crystallographic structure of AChE reveals that it has a narrow 20 Å gorge, containing two binding sites: the catalytic active site (CAS) at the bottom and the peripheral anionic site (PAS) near the entrance of the gorge [8–10]. Hence, inhibitors that bind to either one or two sites could inhibit the AChE. However, current studies indicated that AChE could promote amyloid fibril formation by interaction through the PAS of AChE, giving stable AChE– $A\beta$ complex, which are more toxic than single $A\beta$ peptides alone [11]. For this reason, the dual binding inhibitors, which target both PAS and CAS, have become more promising in AD treatment [12,13]; since they will not only alleviate the cognitive deficit of AD patients by elevating ACh levels but also act as disease-modifying agents delaying amyloid plaque formation [14]. In normal brain, AChE is more active than BuChE and hydrolyzes about 80% of ACh. However, as AD progresses, the activity of AChE decreases, while that of BuChE significantly rises becoming a modulator to regulate ACh levels in cholinergic neurons [15]. Consequently, both enzymes are useful therapeutic targets for AD.

Converging lines of evidence suggest that progressive cerebral deposition of $A\beta$ also plays an important role in the pathogenesis and development of AD, as its accumulation may result in a cascade

* Corresponding author. Tel./fax: +86 25 83271405.

E-mail addresses: cpu_lykong@126.com, lykong@jionline.com (L.-Y. Kong).



Scheme 1. Synthesis of intermediates **4a–m**, **7a–c**. Reagents and conditions: (a) LiHMDS, THF, -78°C to r.t., 4 h; (b) $\text{Br}(\text{CH}_2)_n\text{Br}$ ($n = 2–6$), anhydrous K_2CO_3 , acetone, reflux, 4 h; (c) MeI, anhydrous K_2CO_3 , acetone, reflux, 2 h; (d) SnCl_2 , EtOH, reflux, 1 h; (e) $(\text{CH}_2\text{O})_n$, NaCNBH₃, HOAc, r.t., 3 h; (f) DMF, $\text{CH}_3\text{SO}_2\text{Cl}$, $\text{BF}_3 \cdot \text{Et}_2\text{O}$, r.t. to 90°C ; (g) Triethyl orthoformate, 70% HClO_4 , -20°C to r.t., 8 h, then, H_2O , 100°C , 1 h.

of biochemical events leading to neuronal dysfunction [16]. A β is a proteolytic fragment derived from the amyloid precursor protein (APP), a transmembrane glycoprotein that is usually processed by the enzyme α -secretase to generate in physiological conditions small and soluble peptides [17]. In AD affected brain, amyloidogenic pathway takes place involving the sequential action of β -secretase followed by γ -secretase to generate two predominant A β peptides, either 40 (A β 40) or 42 (A β 42) amino acids in length. This longer form is more prone to aggregate into fibrils, and it makes up the major component of amyloid plaques. Therefore, inhibitors of the A β 42 aggregation may be effective in blocking the progression of the pathology [18].

Recent studies indicate that another hypothesis, called metal hypothesis, may contribute to AD pathology [19]. It is observed that the level of metal ions (Fe, Cu, Zn) in AD patients is 3–7 folds higher than that of healthy individuals [20]. The abnormal accumulation of metals is able to accelerate the formation of A β aggregates and neurofibrillary tangles, which promote inflammation and activate neurotoxic pathways, leading to dysfunction and death of brain cells [21,22]. In addition, studies suggest that redox-active ions like Cu^{2+} and Fe^{2+} are involved in the production of reactive oxygen species (ROS) and oxidative stress which are critical for A β neurotoxicity [23]. Therefore, modulation of such biometals in the brain has been proposed as a potential therapeutic strategy for the treatment of AD.

Due to the pathological complexity found in AD, a single drug that acts on a specific target to produce the desired clinical effects might not be suitable. Thus, multifunctional molecules with two or more complementary biological activities may represent an important advance for the treatment of the disease [24–26]. Herein, our aim is to obtain new multifunctional cholinesterase inhibitors (ChEIs) endowed with addition properties such as lowering the A β aggregation and chelating metals.

Tacrine, the most potent and clinically effective acetylcholinesterase inhibitor (AChEI), was approved by FDA in 1993 [27]. However, it was withdrawn from the market due to its dose-dependent hepatotoxicity [28]. Because of the clinical effectiveness of

acetylcholinesterase inhibitors (AChEIs) in general and the high potency of tacrine in particular, this structure has been widely used for application in hybrid or multitarget compounds in order to obtain potent AChEIs with other pharmacological properties [29,30]. For example, tacrine–melatonin hybrids and tacrine–ferulic acid hybrids have been designed as potent ChEIs with antioxidant properties [31], tacrine–4-oxo-4H-chromene hybrids have been designed as multifunctional agents capable of inhibiting ChE and β -secretase [32], and tacrine–8-hydroxyquinoline hybrids have been designed to exhibit neuroprotective, cholinergic, antioxidant, and copper-complexing properties [33]. Flavonoids, a group of naturally occurring compounds with low molecular weight, have attracted increasingly widespread attention in present-day society, since they possess a wide range of pharmacological properties related to a variety of neurological disorders, such as AChE and BuChE inhibitory activities [34,35], A β fibril formation inhibitory activity [36], free radical scavenging effect [37] and metal-chelating ability [38]. Thus, the design and synthesis of new effective flavonoid derivatives are an interesting strategy for the research on anti-AD drugs.

Very recently, our group has reported the synthesis of tacrine–coumarin hybrids as multifunctional ChEIs against AD [39]. Continuing with our research on various natural products with potential application in the AD field. In this paper, flavonoid was selected to hybridize with tacrine to design a series of new hybrids, exhibiting multifunctional activities. Tacrine for the inhibition of ChE through its binding to the CAS while flavonoid for its metal-chelating, and A β -lowering activities, as well as for its potential interaction with the PAS due to its aromatic character. Since the AChE-CAS is located at the bottom of a deep gorge, we considered connecting tacrine and flavonoid fragments by piperazine side-armed-alkane spacer. These flexible linkers could be lodged by the enzyme cavity, allowing simultaneous interaction between the heteroaromatic fragments and both the CAS and PAS of AChE. Moreover, the linker fragment could establish additional contacts by binding to the aromatic residues of the enzyme mild-gorge through cation– π interactions [40,41].

In this paper we described the synthesis, pharmacological evaluation, and molecular modeling of a series of new tacrine–flavonoid hybrids. The pharmacological evaluations of these new compounds include AChE and BuChE inhibition, the kinetics of enzyme inhibition, self-induced A β aggregation, and metal chelation. Finally, molecular modeling studies were performed to gain insight into the binding mode and structure–activity relationships of new hybrid compounds.

2. Result and discussion

2.1. Chemistry

The key intermediates (**4a–m**, **7a–c**) were synthesized as shown in Scheme 1. Compounds **3a–f** were obtained following a described method [42] and then reacted with α,ω -dibromoalkanes in the presence of potassium carbonate to provide the key intermediates **4a–f** and **4h–k**. The methylation of 5-OH group of **4f** with methyl iodide and potassium carbonate afforded compound **4g**. The free amino derivative **4l** was readily prepared from **4k** by reduction with SnCl₂ in ethanol under reflux condition [43]. Conversion of **4l** to the dimethylamino derivative **4m** was achieved by an efficient method with paraformaldehyde, sodium cyanoborohydride, and acetic acid [44].

Commercially available **1b** was treated with triethyl orthoformate and 70% perchloric acid, followed by hydrolysis in boiling water to afford **5**, which was then treated with dibromopropane to afford **7a** [45]. Compound **7a** was methylated in presence of methyl iodide and potassium carbonate in acetone under reflux condition to gain **7b**. Compound **6** was obtained from **1a** underwent Vilsmeier–Haack formylation and cyclization, and then treated with dibromopropane and potassium carbonate in acetone to afford **7c** [46].

On the other hand, compound **9** was synthesized from anthranilic acid using a previous reported method [47]. The obtained compound **9** was then treated with aminoethanol and 3-amino-1-propano to afford **10a** and **10b**, respectively. Treatment of the **10** with 4-toluene sulfonyl chloride in the presence of triethylamine provided **11**, which were then treated with excess anhydrous piperazine to give **12** (Scheme 2). The obtained compounds **12** were finally reacted with corresponding flavonoid derivatives **4a–m** and **7a–c** to furnish desired compounds **13a–u** (Scheme 3).

All synthesized compounds (**13a–u**) were characterized by IR, ¹H NMR, ¹³C NMR and Mass spectroscopy including HRMS. The IR spectra of compounds showed absorption bands of –NH– stretching vibration at 3345–3445 cm⁻¹. Skeleton vibrations for

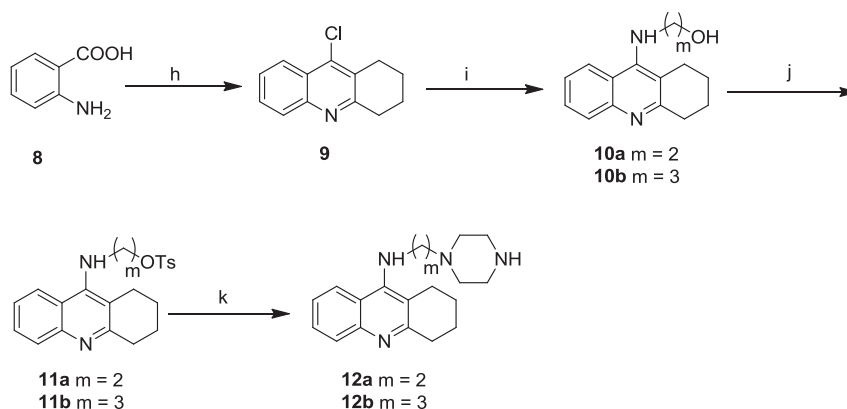
fused and heterocyclic rings appeared in between 1445 and 1602 cm⁻¹. The characteristic strong bands appeared for C=O stretching in flavonoid at 1631–1660 cm⁻¹. The ¹H NMR spectra of all the compounds showed signals for aromatic protons between δ 6.19–8.62 ppm and the –CH₂–O– protons resonated as a triplet between δ 4.08 and 4.12 ppm. The piperazine protons appeared at δ 2.50–2.80 ppm. In the ¹³C NMR spectra, the carbon resonance frequencies of the C=O was at δ 177.0–182.5 ppm. The aromatic carbons appeared at δ 93.3–165.1 ppm and the –CH₂– groups appeared at δ 16.9–66.8 ppm. Moreover, their ESI-MS spectra showed molecular ion [M + H]⁺ peaks further confirming their structure. The molecular formula and elemental composition were confirmed by HRMS. All spectroscopic measurements confirmed the structure and high purity of synthesized compounds.

2.2. Cholinesterase inhibitory activity

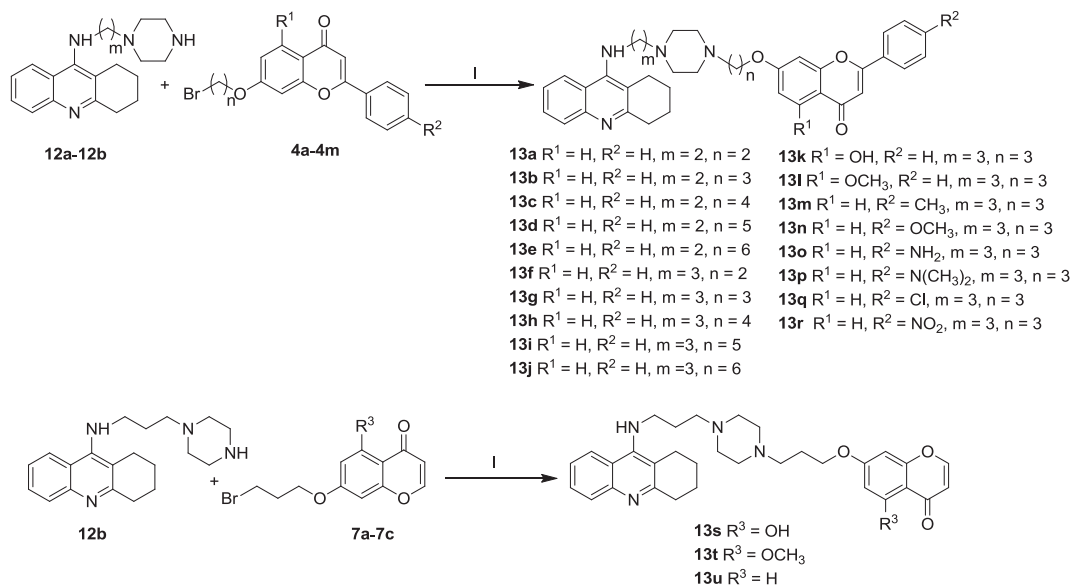
The inhibitory activity of hybrids **13a–u** and relative compound **3a** against AChE (from electric eel) and BuChE (from equine serum) was measured according to the spectrophotometric method of Ellman et al. [48]. For comparison purpose, tacrine and galanthamine were used as reference compounds. The IC₅₀ values of all tested compounds and their selectivity index for AChE over BuChE were summarized in Table 1. From Table 1, it could be seen that all new target compounds showed good inhibitory activity to both ChE with IC₅₀ values ranging from sub-micromolar to nanomolar. Among the target compounds, **13t** (IC₅₀ = 8.4 nM) showed the most potent inhibitory activity for AChE, which was 31- and 318-times stronger than those of the reference compounds tacrine (IC₅₀ = 260 nM) and galanthamine (IC₅₀ = 2670 nM), respectively. In contrast, **13u** exhibited strongest inhibition to BuChE with IC₅₀ value of 25.8 nM, which was 2- and 508-fold more potent than those of tacrine (IC₅₀ = 50.0 nM) and galanthamine (IC₅₀ = 12,700 nM).

From the IC₅₀ value of compounds **13a–j**, it appeared that the proper tether for the linker between the two anchoring groups, tacrine and flavonoid, seemed to be six ($m + n = 6$), especially $m = n = 3$. It also concluded that the variation of chain length for the inhibitors had more influence on their inhibition of AChE than BuChE. A possible reason is conformational difference between these two enzymes. By contrast, BuChE does not have a function peripheral site, and the active site of BuChE is wider than that of AChE. Therefore, BuChE has less restriction to inhibitors with varying linker length.

With the optimal length of the linker ($m = n = 3$) in hand, we planned to introduce different substituents with varying electronic



Scheme 2. Synthesis of intermediates **12**. Reagents and conditions: (h) POCl₃, cyclohexanone, reflux, 4h; (i) NH₂(CH₂)_mOH, $m = 2-3$, 160 °C, 8 h; (j) PTSC, TEA, DMAP, CH₂Cl₂, 0 °C to r.t., 4 h; (k) anhydrous piperazine, DMF, 80 °C, 2 h.



Scheme 3. Synthesis of tacrine–flavonoid hybrids **13a–u**. Reagents and conditions: (I) intermediates **4a–m**, **7a–c**, anhydrous K₂CO₃, CH₃CN, reflux, 8 h.

properties to the flavonoid. First of all, hydroxy and methoxy group was introduced to the 5-position of flavone moiety producing **13k–l** that resulted in a slight increase in AChE inhibition, but no significant influence on BuChE inhibition. Moreover, the inhibitory activity of target compounds was sensitive to the substituents at 4'-position of flavone ring. As shown in Table 1, **13m–p** possessing an electron-donating group at 4'-position of the B ring in flavone moiety showed a decreased AChE inhibitory activity, while **13q–r** possessing an electron-drawing group showed an increased AChE inhibitory activity. By contrast, both electron-donating group and electron-drawing group showed a slight decrease in BuChE

inhibition. These results implied that an electron-drawing group at 4'-position of the B ring seemed beneficial to AChE inhibitory activity, and made it more selective to AChE inhibitory activity.

To extend the series of the hybrids, compounds **13s–u** without the B ring in flavone moiety were synthesized. Interestingly, it was found that both AChE and BuChE inhibitory activities of these compounds were increased more remarkably than **13g**. For example, the inhibitory activities of **13u** for AChE and BuChE (IC₅₀ = 10.3 nM for AChE; IC₅₀ = 25.8 nM for BuChE) were 15-fold and 8-fold more potent, respectively, than those of **13g** (IC₅₀ = 153 nM for AChE; IC₅₀ = 208 nM for BuChE). It suggested

Table 1
Inhibition of ChEs activity and selectivity index of compounds.

Compound	R ¹	R ²	R ³	m	n	IC ₅₀ (nM)		Selectivity index ^c
						AChE ^a	BuChE ^b	
3a						85,000 ± 50	>100,000	>1.2
13a	H	H		2	2	481 ± 8	520 ± 8	1.1
13b	H	H		2	3	624 ± 14	311 ± 15	0.5
13c	H	H		2	4	268 ± 12	197 ± 7	0.7
13d	H	H		2	5	568 ± 12	258 ± 10	0.5
13e	H	H		2	6	717 ± 15	289 ± 12	0.4
13f	H	H		3	2	416 ± 12	266 ± 8	0.6
13g	H	H		3	3	153 ± 8	208 ± 5	1.4
13h	H	H		3	4	547 ± 15	317 ± 15	0.6
13i	H	H		3	5	594 ± 13	423 ± 7	0.7
13j	H	H		3	6	848 ± 15	414 ± 8	0.5
13k	OH	H		3	3	133 ± 5	558 ± 6	4.2
13l	CH ₃ O	H		3	3	57.7 ± 4.5	360 ± 8	6.2
13m	H	CH ₃		3	3	316 ± 15	573 ± 14	1.8
13n	H	CH ₃ O		3	3	417 ± 30	655 ± 8	1.6
13o	H	NH ₂		3	3	336 ± 12	685 ± 5	2.0
13p	H	N(CH ₃) ₂		3	3	230 ± 6	845 ± 10	3.7
13q	H	Cl		3	3	40.1 ± 0.3	994 ± 10	24.8
13r	H	NO ₂		3	3	75.0 ± 2.5	460 ± 8	6.1
13s			OH	3	3	15.4 ± 0.5	45.0 ± 3.0	2.9
13t			CH ₃ O	3	3	8.4 ± 0.8	35.0 ± 0.5	4.2
13u			H	3	3	10.3 ± 0.5	25.8 ± 0.8	2.5
Tacrine						260 ± 8	50 ± 3	0.2
Galantamine						2670 ± 15	12700 ± 2	4.76

^a Inhibitor concentration (mean ± SEM of three experiments) required for 50% inactivation of AChE.

^b Inhibitor concentration (mean ± SEM of three experiments) required for 50% inactivation of BuChE.

^c Selectivity index = IC₅₀ (BuChE)/IC₅₀ (AChE).

Table 2
Inhibition of A β (1–42) self-induced aggregation of compounds.

Compound	R ¹	R ²	R ³	m	n	A β (1–42) aggregation inhibition (%) ^a	A β (1–42) IC ₅₀ (μ M) ^b
3a						27.2 \pm 0.9	n.t. ^c
13a	H	H		2	2	54.1 \pm 3.0	16.8 \pm 2.1
13b	H	H		2	3	59.1 \pm 1.4	13.7 \pm 2.3
13c	H	H		2	4	53.7 \pm 1.1	16.4 \pm 1.6
13d	H	H		2	5	65.4 \pm 2.0	12.8 \pm 0.7
13e	H	H		2	6	63.3 \pm 1.8	14.2 \pm 1.2
13f	H	H		3	2	70.0 \pm 1.9	9.8 \pm 1.1
13g	H	H		3	3	58.0 \pm 1.4	14.9 \pm 2.0
13h	H	H		3	4	53.4 \pm 2.0	17.3 \pm 2.1
13i	H	H		3	5	62.5 \pm 2.4	13.2 \pm 1.9
13j	H	H		3	6	63.0 \pm 1.8	13.5 \pm 0.4
13k	OH	H		3	3	79.1 \pm 1.4	6.5 \pm 1.9
13l	CH ₃ O	H		3	3	68.7 \pm 3.3	9.6 \pm 0.7
13m	H	CH ₃		3	3	13.4 \pm 0.6	n.t. ^c
13n	H	CH ₃ O		3	3	10.9 \pm 0.2	n.t. ^c
13o	H	NH ₂		3	3	9.0 \pm 0.3	n.t. ^c
13p	H	N(CH ₃) ₂		3	3	12.2 \pm 0.5	n.t. ^c
13q	H	Cl		3	3	48.9 \pm 1.2	n.t. ^c
13r	H	NO ₂		3	3	61.1 \pm 1.2	14.1 \pm 1.2
13s			OH	3	3	85.3 \pm 2.7	4.8 \pm 0.6
13t			CH ₃ O	3	3	62.0 \pm 1.7	12.6 \pm 1.4
13u			H	3	3	67.4 \pm 3.8	11.5 \pm 1.7
Curcumin						43.5 \pm 2.9	20.3 \pm 1.2

^a Inhibition of A β (1–42) self-induced aggregation, the thioflavin-T fluorescence method was used, the mean \pm SD of at least three independent experiments and the measurements were carried out in the presence of 20 μ M compounds the presence of 20 μ M compounds.

^b The IC₅₀ (μ M) values shown in this table are the mean \pm SD of three experiments.

^c n.t. means not tested.

that the high hydrophobicity and/or the steric hindrance of the phenyl ring might be not favorable for ChE inhibition.

2.3. Inhibition of A β (1–42) self-induced aggregation

All compounds tested their activities for both ChE inhibition were also tested for their ability to inhibit A β (1–42) self-induced aggregation by using a thioflavin-T based fluorometric assay [49,50]. Curcumin (Cur), a known active natural product for the inhibition of A β (1–42) self-aggregation, was used as reference compound and the results were summarized in Table 2 and showed in Fig. 1. From the results, it could be seen that most hybrids exhibited moderate-to-good potencies (9.0–85.3% at 20 μ M) compared to that of curcumin (43.5% at 20 μ M). The complete dose–response curves were obtained by assaying those

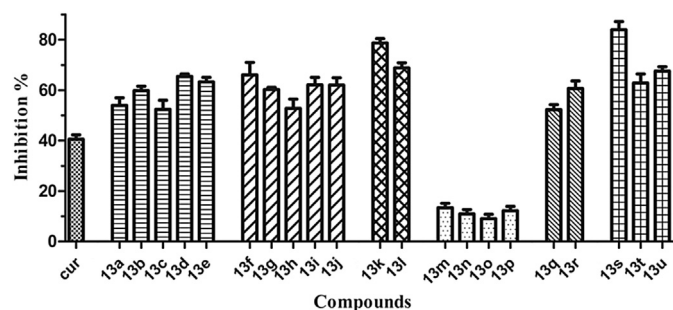


Fig. 1. Inhibition of A β (1–42) self-induced aggregation by compounds (**13a–u**) comparing with that of curcumin. The thioflavin-T fluorescence method was used and the measurements were carried out in the presence of 20 μ M test compound. The mean \pm SD values from three independent experiments were shown.

Lineweaver-Burk plot
AChE inhibition by **13s**

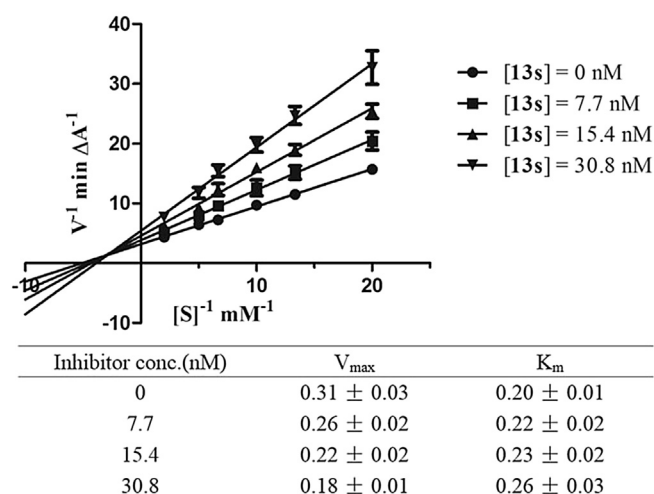


Fig. 2. Lineweaver–Burk plots resulting from subvelocity curve of AChE activity with different substrate concentrations (0.05–0.50 mM) in the absence and presence of 7.7, 15.4, 30.8 nM **13s**. The V_{max} and K_m values shown in this table are the mean \pm SD of three experiments.

compounds with inhibition rate greater than 50%. The result indicated that **13s** (IC₅₀ = 4.8 μ M) was the most potent inhibitor of A β (1–42) among the series of compounds featuring a hydroxyl group at the 5 position of flavonoid moiety and without the B ring at the 2 position. From the inhibition values of compounds **13a–j**, it appeared that the linker length didn't play a role in determining the inhibition of A β (1–42) self-aggregation, since no significant change of the percentages of inhibition was observed along with the lengthening of the spacer length. In contrast, compounds **13m–p** only showed the percentages of inhibition ranging from 9.0 to 13.4%, nearly 4-fold lower than that of the curcumin. These results indicated that, similarly to ChE inhibition, an electron-donating group at 4'-position of flavone moiety might not be favorable for inhibition of A β (1–42) self-aggregation. Compounds with a hydroxyl group or methoxy group at the 5 position of the A ring, exhibited good inhibitory activities (**13k–l**, **13s–t**, from 4.8 to 12.6 μ M). These results implied that an electron-donating group at the 5 position of A ring seemed to be beneficial to A β (1–42) self-aggregation inhibitory activity.

2.4. Kinetic study of ChE inhibition

To gain information on the mechanism of inhibition, the potent inhibitor **13s** was selected for kinetic studies because of its total performance with regard to cholinesterase inhibition and self-induced A β (1–42) aggregation inhibition. The type of inhibition was elucidated from the analysis of Lineweaver–Burk plots, which were reciprocal rates versus reciprocal substrate concentrations for the different inhibitor concentrations resulting from the substrate–velocity curves for ChE. For AChE, the plot showed both increased slopes (decreased V_{max}, from 0.31 to 0.18) and intercepts (higher K_m, from 0.20 to 0.26) at increasing concentration of the inhibitor (Fig. 2). This pattern indicated a mixed-type inhibition and therefore revealed that compound **13s** might be able to bind to CAS as well as PAS of AChE. In contrast, a different plot for BuChE was obtained, showing different K_m (from 0.15 to 0.41) and constant V_{max} in different inhibitor concentrations (Fig. 3). This suggested a competitive inhibition, revealing that these

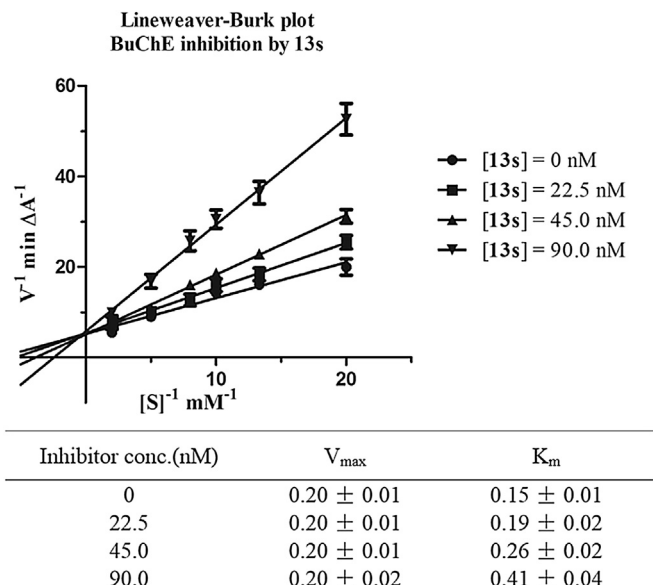


Fig. 3. Lineweaver–Burk plots resulting from subvelocity curve of BuChE activity with different substrate concentrations (0.05–0.50 mM) in the absence and presence of 22.5, 45.0, 90.0 nM **13s**. The V_{\max} and K_m values shown in this table are the mean \pm SD of three experiments.

compounds compete for the same binding site (CAS) as the substrate acetylcholine.

2.5. Molecular modeling studies

To further study the interaction mode of compound **13s** for AChE, molecular docking study was performed using software package MOE 2008.10. The X-ray crystal structure of the TcAChE complex with bis (7)–tacrine (PDB ID 2CKM) was applied to build the starting model of AChE. As showed in Fig. 4, tacrine moiety of **13s** was bound to the CAS of AChE, it being stacked against the phenyl ring of Phe 330 and the indole ring of Trp 84 with the ring-to-ring distance of 3.44 and 3.68 Å, respectively. The flavonoid ring interacted with the indole ring of Trp 279 and Tyr70 of PAS via π – π stacking interactions with the distance of 4.24 and 5.05 Å, respectively. As we expected, the piperazine could bind to the mid-gorge binding site of AChE through a cation– π interaction (5.45 Å) between its protonated nitrogen atom and Tyr 334 in the middle gorge. All these results clearly indicated that compound **16s** could simultaneously bind to CAS, PAS and mid-gorge binding site of AChE, thereby demonstrating rationality of our molecular design.

As known, flavonoids with free 5-hydroxyl and 4-keto groups may use this 5-hydroxy-4-keto site for metal chelation. Compounds **13k** and **13s** may have metal-chelating ability since they all have the 5-hydroxy-4-keto site. In addition, **13k** and **13s** showed potent inhibitory activities toward ChE and A β (1–42) self-induced aggregation. They had fine IC_{50} values in micromole range ($IC_{50} = 6.5 \mu\text{M}$ for **13k**, $IC_{50} = 4.8 \mu\text{M}$ for **13s**) for inhibition of self-aggregation of A β , and the inhibitory activities of **13s** for AChE and BuChE ($IC_{50} = 15.4 \text{ nM}$ for AChE; $IC_{50} = 45.0 \text{ nM}$ for BuChE) were 8.6 and 12-fold more potent than those of **13k** ($IC_{50} = 133 \text{ nM}$ for AChE; $IC_{50} = 558 \text{ nM}$ for BuChE). Compound **13s** might be more potent than **13k** due to their ChE inhibitory activity. However, we wanted to achieve a balanced multitarget profile rather than just a highly potent ChE inhibitor. That IC_{50} values for ChE and A β aggregation inhibition in multifunctional compound were close would be superior to compound with large difference of them.

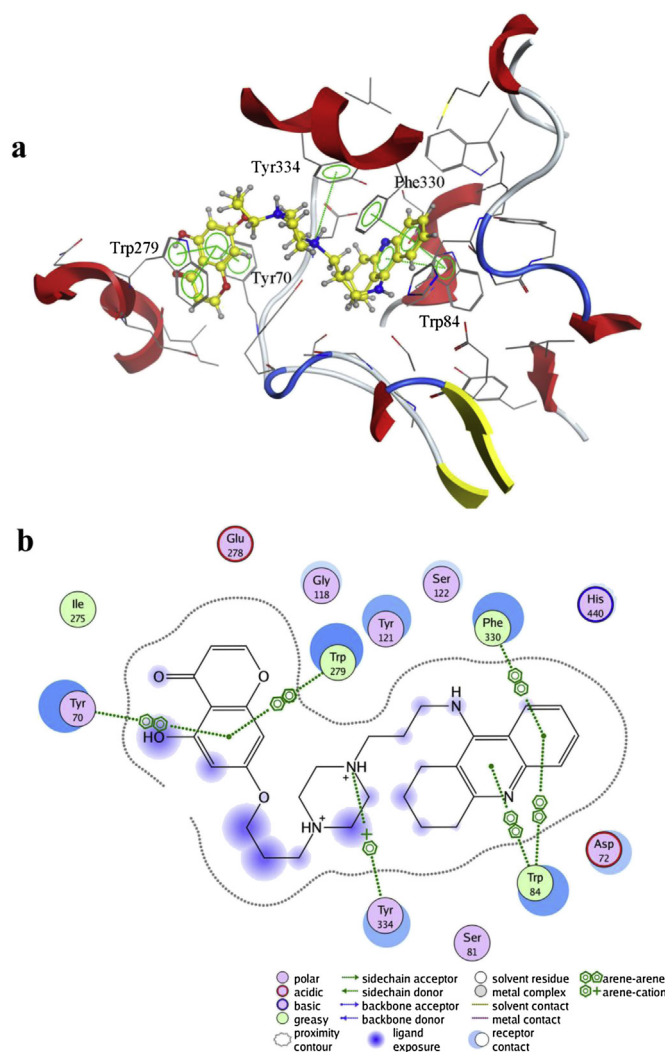


Fig. 4. (a) 3D docking model of compound **13s** with TcAChE. Atom colors: yellow – carbon atoms of **13s**, gray – carbon atoms of residues of TcAChE, dark blue – nitrogen atoms, red – oxygen atoms. The dashed lines represent the interactions between the protein and the ligand. (b) 2D schematic diagram of docking model of compound **13s** with TcAChE. The figure was prepared using the ligand interactions application in MOE. (For interpretation of the references to color in this figure legend, the reader is referred to the web version of this article.)

From this point of view, compound **13k** could be more effective due to its anti-A β activity which was almost the same as activity of **13s** and had much higher IC_{50} values for ChE inhibition.

2.6. Metal chelating effect

To further study, the chelating effect of **13k** for metals such as Cu^{2+} and Fe^{2+} in methanol was studied by UV–vis spectrometry with wavelength ranging from 200 to 500 nm [51,52]. In Fig. 5a, UV–vis spectra of **13k** at increasing Cu^{2+} concentrations were shown as an example. The increase in absorbance, which could be better estimated by an inspection of the differential spectra (Fig. 5b), indicated that there was an interaction between Cu^{2+} and **13k**. The similar behavior was also observed when using Fe^{2+} . These observations indicated that **13k** could effectively chelate Cu^{2+} and Fe^{2+} , and thereby could serve as metal chelator in treating AD. The ratio of ligand/metal ion in the complex was investigated by mixing the fix amount metal ion with increasing ligand; it was

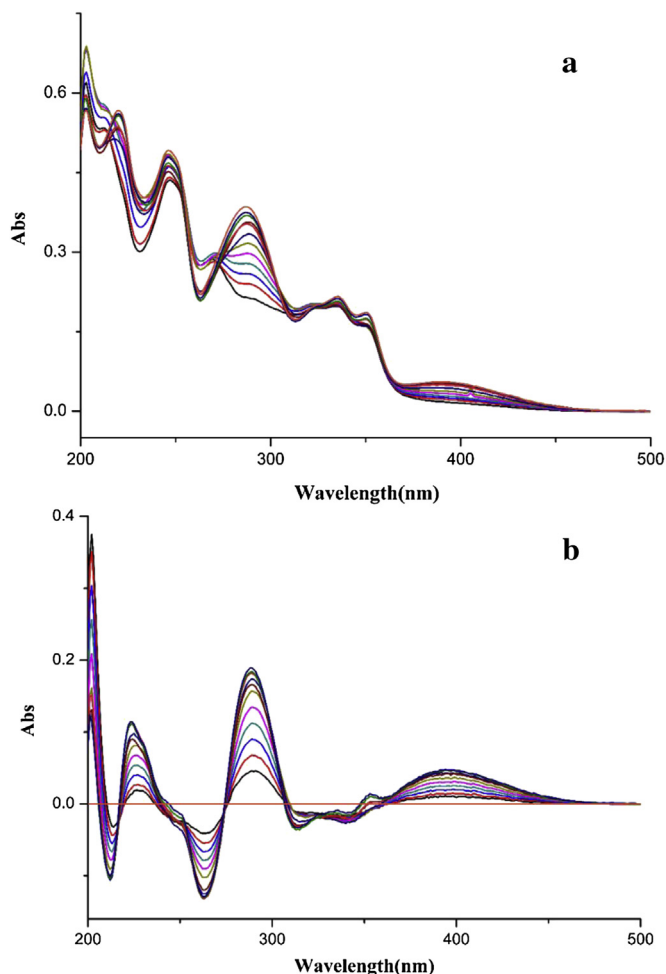


Fig. 5. (a) UV–vis (200–500 nm) absorption spectra of **13k** (25 μM) in methanol after addition of ascending amounts of CuCl₂ (2–50 μmol/L). (b) The differential spectra due to **13k**–Cu²⁺ complex formation obtained by numerical subtraction from the above spectra of those of Cu²⁺ and **13k** at the corresponding concentrations.

possible to observe that the maximum intensity of difference spectra was reached at 1:1 ratio, which was taken as an indication of the stoichiometry of the complex.

2.7. SH-SY5Y neuroblastoma cell toxicity

On basis of the screening results above, the most potent compound **13k** was selected to further examine the potential toxicity effect on the human neuroblastoma cell line SH-SY5Y [33,53]. After exposing the cells to this compound for 24 h, the cell viability was evaluated by the 3-(4,5-dimethylthiazol-2-yl)-2,5-diphenyltetrazolium (MTT) assay. The result indicated that **13k** did not show significant effect on cell viability at 1–50 μM (1 μM: 97.3 ± 14.7%; 5 μM: 96.5 ± 17.5%; 10 μM: 94.4 ± 13.6%; 25 μM: 92.7 ± 10.4%; 50 μM: 90.1 ± 8.5%). This suggested that **13k** was nontoxic to SH-SY5Y cells and might be a suitable multifunctional ChE inhibitor for treating AD.

2.8. Hepatotoxicity studies

The main disadvantage of tacrine is the high hepatotoxicity which can be prevented with free radical scavengers [54]. To determine whether our compounds had hepatotoxicity in comparison to tacrine, **13k** was selected for the assay with adult mice.

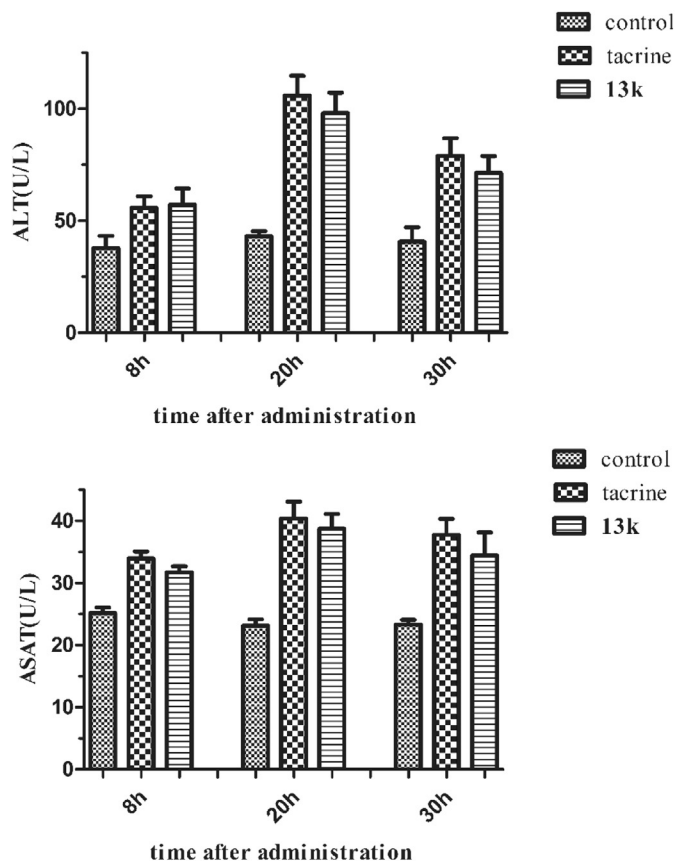


Fig. 6. ALT and ASAT activity after the administration of tacrine and **13k**. Values are expressed as mean ± SEM ($n = 8–9$, t test, compared to control of the same time after administration, $p^* \leq 0.05$, $p^{**} \leq 0.01$).

After being treated with tacrine, **13k**, the heparinized serum of mice was obtained after different times and the levels of aspartate aminotransferase (ASAT) and alanine aminotransferase (ALT) were determined. In comparison to the control, tacrine caused significant hepatotoxicity, as indicated by the increased activity of ASAT and ALT. From the results, it appears that **13k** may be safer than tacrine, but not obviously (Fig. 6).

The antioxidant activities of **13a–u** using a radical scavenging assay (DPPH assay) had been tested. All the compounds showed tiny antioxidant activities (at the concentration 2 mM, the activities in % of compounds **13a–u** were less than 36%). This explained the weak hepatoprotective activity of **13a–u**. In future studies, we should introduce more free phenolic hydroxyl groups in the structure to improve the antioxidant activity, and this might be beneficial for the hepatoprotective activity.

3. Conclusion

In conclusion, a series of tacrine–flavonoid hybrids had been designed and synthesized as multifunctional ChEIs. Most of compounds inhibited ChE in the nanomolar range in vitro effectively. Kinetic and molecular modeling studies also indicated the compounds were mixed-type inhibitors, binding simultaneously to active, peripheral and mid-gorge sites of AChE. Most of the hybrids exhibited higher percentages of inhibition than the reference compound curcumin in inhibition of Aβ (1–42) aggregation assay. Among them, **13k** and **13s** showed moderate metal-chelating ability since they had 5-hydroxy-4-keto site. The weaker ChE inhibition potencies and the concomitant nearly equipotent anti-

amyloid activities of **13k** with respect to **13s** resulted in a more balanced biological profile against both targets. Compound **13k** could be more effective, and it was selected as potent lead compound for further study. In the cell toxicity assay, **13k** showed nontoxic to SH-SY5Y cell at 1–50 μM . Altogether, the multifunctional effects of the new hybrids qualified them as potential anti-AD drug candidates and **13k** might be considered as a promising lead compound for AD treatment.

4. Experimental section

4.1. Chemistry

All chemicals (reagent grade) used were purchased from Sino-pharm Chemical Reagent Co., Ltd. (China). Reaction progress was monitored using analytical thin layer chromatography (TLC) on precoated silica gel GF₂₅₄ (Qingdao Haiyang Chemical Plant, Qingdao, China) plates and the spots were detected under UV light (254 nm). Melting point was measured on an XT-4 micromelting point instrument and uncorrected. IR (KBr-disc) spectra were recorded by Bruker Tensor 27 spectrometer. ¹H NMR and ¹³C NMR spectra were measured on a Bruker ACF-500 spectrometer at 25 °C and referenced to TMS. Chemical shifts are reported in ppm (δ) using the residual solvent line as internal standard. Splitting patterns are designed as s, singlet; d, doublet; t, triplet; m, multiplet. The purity of all compounds was confirmed to be higher than 95% through analytical HPLC performed with Agilent 1200 HPLC System (Supporting information, Table S1). Mass spectra were obtained on a MS Agilent 1100 Series LC/MSD Trap mass spectrometer (ESI-MS) and a Mariner ESI-TOF spectrometer (HRESIMS), respectively. Column chromatography was performed on silica gel (90–150 μm ; Qingdao Marine Chemical Inc.)

4.1.1. General procedures for the preparation of intermediate **3a–f**

A solution of lithium bis(trimethyl)silyl amide (LiHMDS) in THF (1 mol/L, 40 mmol) was added to a well-stirred solution of **1** (10 mmol) in THF under a nitrogen atmosphere at –78 °C over 15 min. The reaction mixture was stirred at –78 °C for 3 h and a solution of the appropriate benzoyl chloride (10 mmol) in THF (20 mL) was added over 10 min. Stirring was continued for 1 h at –78 °C and at room temperature for 4 h. Then the reaction mixture was poured into a mixture of ice water (250 mL) and HCl (10 mL). It was extracted with CH₂Cl₂ (3 \times 25 mL) and the combined extracts were dried over anhydrous Na₂SO₄. The solvent was evaporated and the residue mixed with glacial acetic acid (50 mL) and H₂SO₄ (0.25 mL) and heated at 100 °C for 1 h. Water was added and the product was filtered, washed with water and crystallized from acetone/petrol ether.

4.1.2. 5,7-Dihydroxy-chromen-4-one (**5**)

BF₃·Et₂O (7.6 mL, 60 mmol) was added drop wise to a solution of acetylphloroglucinol **1b** (2.8 g, 15 mmol) in anhydrous DMF (25 mL) for 15 min. A solution of methanesulfonyl chloride (3.5 mL, 45 mmol) in anhydrous DMF (10 mL) was added to the mixture, which was heated at 90 °C for 3 h, cooled, and slowly poured into ice-water (50 mL) under strong stirring. The crude product was filtered off and washed with water to afford the dark yellow solid. The crude product was purified by silica gel chromatography with ethyl acetate and petroleum ether (1:3) to afford **5** as yellow solid. Yield 91.0%, ESI-MS m/z : 179.0 [M + H]⁺.

4.1.3. 7-Hydroxychromone (**6**)

Perchloric acid (70%, 0.7 mL) was slowly added into a suspension of 2,4-dihydroxyacetophenone **1a** (1.0 g, 6.7 mmol) in triethyl orthoformate (6 mL) with stirring. The mixture was stirred

continuously until it cooled to room temperature. Anhydrous diethyl ether (18 mL) was added to precipitate the intermediate oxonium perchlorate salt, which was subsequently hydrolyzed in hot water (30 mL) to provide **6** as a brown solid. Yield 65.0%, ESI-MS m/z : 163.0 [M + H]⁺.

4.1.4. General procedures for the preparation of intermediate **4a–f**, **4h–k**, **7a**, and **7c**

A mixture of **3a–f/5–6** (5 mmol) with suitable α,ω -dibromoalkanes (50 mmol) and anhydrous K₂CO₃ (1.4 g, 10 mmol) in acetone (15 mL) was refluxed under stirring for 4 h. After cooling, the reaction mixture was filtered and the filtrate was evaporated under reduced pressure. The obtained residue was purified by silica gel chromatography with hexane/acetone (20:1) as eluent to give compounds **4a–f**, **4h–k**, **7a**, and **7c**.

4.1.4.1. 7-(2-Bromoethoxy)-2-phenyl-4H-chromen-4-one (**4a**). Intermediate **3a** was treated with 1,2-dibromoethane according to the general procedure to give the desired product **4a** as a light yellow solid, yield 85.0%; ¹H NMR (500 MHz, DMSO-*d*₆) δ 8.10 (dd, $J = 6.0, 2.0$ Hz, 2H), 7.96 (d, $J = 8.5$ Hz, 1H), 7.65–7.54 (m, 3H), 7.38 (d, $J = 2.5$ Hz, 1H), 7.10 (dd, $J = 8.5, 2.0$ Hz, 1H), 6.97 (s, 1H), 4.51 (t, $J = 5.5$ Hz, 2H), 3.88 (t, $J = 5.5$ Hz, 2H); ESI-MS m/z : 345.0 [M + H]⁺.

4.1.4.2. 7-(3-Bromopropoxy)-2-phenyl-4H-chromen-4-one (**4b**). Intermediate **3a** was treated with 1,3-dibromopropane according to the general procedure to give the desired product **4b** as a light yellow solid, yield 88.1%; ¹H NMR (500 MHz, DMSO-*d*₆) δ 8.11–8.09 (m, 2H), 7.97 (d, $J = 8.5$ Hz, 1H), 7.61–7.56 (m, 3H), 7.37 (d, $J = 2.0$ Hz, 1H), 7.09 (dd, $J = 8.5, 2.0$ Hz, 1H), 6.97 (s, 1H), 4.27 (t, $J = 6.0$ Hz, 2H), 3.70 (t, $J = 6.5$ Hz, 2H), 2.34–2.31 (m, 2H); ESI-MS m/z : 359.0 [M + H]⁺.

4.1.4.3. 7-(4-Bromobutoxy)-2-phenyl-4H-chromen-4-one (**4c**). Intermediate **3a** was treated with 1,4-dibromobutane according to the general procedure to give the desired product **4c** as a light yellow solid, yield 85.5%; ¹H NMR (500 MHz, DMSO-*d*₆) δ 8.10–8.08 (m, 2H), 7.94 (d, $J = 8.5$ Hz, 1H), 7.61–7.56 (m, 3H), 7.33 (d, $J = 2.0$ Hz, 1H), 7.06 (dd, $J = 8.5, 2.0$ Hz, 1H), 6.96 (s, 1H), 4.19 (t, $J = 6.0$ Hz, 2H), 3.63 (t, $J = 6.5$ Hz, 2H), 2.01–1.97 (m, 2H), 1.93–1.90 (m, 2H); ESI-MS m/z : 373.0 [M + H]⁺.

4.1.4.4. 7-((5-Bromopentyl)oxy)-2-phenyl-4H-chromen-4-one (**4d**). Intermediate **3a** was treated with 1,5-dibromopentane according to the general procedure to give the desired product **4d** as a light yellow solid, yield 78.0%; ¹H NMR (500 MHz, DMSO-*d*₆) δ 8.10 (m, 2H), 7.94 (d, $J = 8.5$ Hz, 1H), 7.61–7.58 (m, 3H), 7.34 (d, $J = 2.0$ Hz, 1H), 7.07 (dd, $J = 8.5, 2.0$ Hz, 1H), 6.97 (s, 1H), 4.16 (t, $J = 6.5$ Hz, 2H), 3.58 (t, $J = 6.5$ Hz, 2H), 1.93–1.87 (m, 2H), 1.85–1.79 (m, 2H), 1.61–1.54 (m, 2H); ESI-MS m/z : 387.0 [M + H]⁺.

4.1.4.5. 7-((6-Bromohexyl)oxy)-2-phenyl-4H-chromen-4-one (**4e**). Intermediate **3a** was treated with 1,6-dibromohexane according to the general procedure to give the desired product **4e** as a light yellow solid, yield 75.5%; ¹H NMR (500 MHz, DMSO-*d*₆) δ 8.10 (m, 2H), 7.94 (d, $J = 9.0, 2.0$ Hz, 2H), 7.61–7.56 (m, 3H), 7.33 (d, $J = 2.0$ Hz, 1H), 7.06 (dd, $J = 9.0, 2.0$ Hz, 1H), 6.97 (s, 1H), 4.15 (t, $J = 6.5$ Hz, 2H), 3.54 (t, $J = 6.5$ Hz, 2H), 1.88–1.75 (m, 4H), 1.52–1.40 (m, 4H); ESI-MS m/z : 401.1 [M + H]⁺.

4.1.4.6. 7-(3-Bromopropoxy)-5-hydroxy-2-phenyl-4H-chromen-4-one (**4f**). Intermediate **3b** was treated with 1,3-dibromopropane according to the general procedure to give the desired product **4f** as a light yellow solid, yield 70.5%; ¹H NMR (500 MHz, DMSO-*d*₆) δ 12.82 (s, 1H), 8.17–8.12 (m, 2H), 7.67–7.60 (m, 3H), 7.07 (s, 1H),

6.88 (d, $J = 2.0$ Hz, 1H), 6.44 (d, $J = 2.0$ Hz, 1H), 4.25 (t, $J = 6.0$ Hz, 2H), 3.70 (t, $J = 6.5$ Hz, 2H), 2.33–2.30 (m, 2H); ESI-MS m/z : 375.0 $[M + H]^+$.

4.1.4.7. 7-(3-Bromopropoxy)-2-(*p*-tolyl)-4H-chromen-4-one (4h). Intermediate **3c** was treated with 1,3-dibromopropane according to the general procedure to give the desired product **4h** as a light yellow solid, yield 72.5%; $^1\text{H NMR}$ (500 MHz, DMSO- d_6) δ 8.01–7.99 (m, 2H), 7.94 (d, $J = 8.5$ Hz, 1H), 7.40–7.37 (m, 3H), 7.08 (dd, $J = 9.0$, 2.5 Hz, 1H), 6.92 (s, 1H), 4.26 (t, $J = 6.0$ Hz, 2H), 3.70 (t, $J = 6.5$ Hz, 2H), 2.40 (s, 3H), 2.33–2.30 (m, 2H); ESI-MS m/z : 373.0 $[M + H]^+$.

4.1.4.8. 7-(3-Bromopropoxy)-2-(4-methoxyphenyl)-4H-chromen-4-one (4i). Intermediate **3d** was treated with 1,3-dibromopropane according to the general procedure to give the desired product **4i** as a light yellow solid, yield 75.0%; $^1\text{H NMR}$ (500 MHz, DMSO- d_6) δ 8.08–8.06 (m, 2H), 7.94 (d, $J = 9.0$ Hz, 1H), 7.36 (d, $J = 2.5$ Hz, 1H), 7.13–7.12 (m, 2H), 7.08 (dd, $J = 9.0$, 2.5 Hz, 1H), 6.87 (s, 1H), 4.26 (t, $J = 6.0$ Hz, 2H), 3.87 (s, 3H), 3.71 (t, $J = 6.5$ Hz, 2H), 2.36–2.28 (m, 2H); ESI-MS m/z : 389.0 $[M + H]^+$.

4.1.4.9. 7-(3-Bromopropoxy)-2-(4-chlorophenyl)-4H-chromen-4-one (4j). Intermediate **3e** was treated with 1,3-dibromopropane according to the general procedure to give the desired product **4j** as a light yellow solid, yield 82.3%; $^1\text{H NMR}$ (500 MHz, DMSO- d_6) δ 8.15–8.13 (m, 2H), 7.97 (d, $J = 9.0$ Hz, 1H), 7.67–7.65 (m, 2H), 7.39 (d, $J = 2.5$ Hz, 1H), 7.09 (dd, $J = 9.0$, 2.5 Hz, 1H), 7.01 (s, 1H), 4.27 (t, $J = 6.0$ Hz, 2H), 3.70 (t, $J = 6.5$ Hz, 2H), 2.36–2.31 (m, 2H); ESI-MS m/z : 393.0 $[M + H]^+$.

4.1.4.10. 7-(3-Bromopropoxy)-2-(4-nitrophenyl)-4H-chromen-4-one (4k). Intermediate **3f** was treated with 1,3-dibromopropane according to the general procedure to give the desired product **4k** as a yellow solid, yield 76.5%; $^1\text{H NMR}$ (500 MHz, DMSO- d_6) δ 8.39–8.38 (m, 4H), 7.97 (d, $J = 9.0$ Hz, 1H), 7.42 (d, $J = 2.5$ Hz, 1H), 7.18 (s, 1H), 7.12 (dd, $J = 9.0$, 2.5 Hz, 1H), 4.28 (t, $J = 6.0$ Hz, 2H), 3.71 (t, $J = 6.5$ Hz, 2H), 2.35–2.32 (m, 2H); ESI-MS m/z : 404.0 $[M + H]^+$.

4.1.4.11. 7-(3-Bromopropoxy)-5-hydroxy-4H-chromen-4-one (7a). Intermediate **5** was treated with 1,3-dibromopropane according to the general procedure to give the desired product **7a** as a yellow solid, yield 70.5%; $^1\text{H NMR}$ (500 MHz, DMSO- d_6) δ 12.70 (s, 1H), 8.27 (d, $J = 6.0$ Hz, 1H), 6.66 (d, $J = 2.5$ Hz, 1H), 6.42 (d, $J = 2.5$ Hz, 1H), 6.35 (d, $J = 6.0$ Hz, 1H), 4.20 (t, $J = 6.0$ Hz, 2H), 3.66 (t, $J = 6.5$ Hz, 2H), 2.29–2.24 (m, 2H); ESI-MS m/z : 299.0 $[M + H]^+$.

4.1.4.12. 7-(3-Bromopropoxy)-4H-chromen-4-one (7c). Intermediate **6** was treated with 1,3-dibromopropane according to the general procedure to give the desired product **7c** as a yellow solid, yield 82.5%; $^1\text{H NMR}$ (500 MHz, DMSO- d_6) δ 8.12 (d, $J = 9.0$ Hz, 1H), 7.91 (d, $J = 6.0$ Hz, 1H), 6.98 (dd, $J = 8.5$, 2.0 Hz, 1H), 6.86 (d, $J = 2.0$ Hz, 1H), 6.30 (d, $J = 6.0$ Hz, 1H), 4.21 (t, $J = 5.5$ Hz, 2H), 3.62 (t, $J = 6.5$ Hz, 2H), 2.40–2.35 (m, 2H); ESI-MS m/z : 283.0 $[M + H]^+$.

4.1.5. General procedures for the preparation of intermediate **4g** and **7b**

A mixture of **4f/7a** (5 mmol) with MeI (1.4 g, 10 mmol) and anhydrous K_2CO_3 (1.4 g, 10 mmol) in acetone (15 mL) was refluxed under stirring for 2 h. After cooling, the reaction mixture was filtered and the filtrate was evaporated under reduced pressure. The obtained residue was purified by silica gel chromatography with hexane/acetone (20:1) as eluent to give compounds **4g** and **7b**.

4.1.5.1. 7-(3-Bromopropoxy)-5-methoxy-2-phenyl-4H-chromen-4-one (4g). Intermediate **4f** was treated with MeI according to the

general procedure to give the desired product **4g** as a yellow solid, yield 65.0%; $^1\text{H NMR}$ (500 MHz, DMSO- d_6) δ 8.06–8.04 (m, 2H), 7.61–7.53 (m, 3H), 6.92 (d, $J = 2.5$ Hz, 1H), 6.78 (s, 1H), 6.54 (d, $J = 2.5$ Hz, 1H), 4.25 (t, $J = 6.0$ Hz, 2H), 3.84 (s, 3H), 3.70 (t, $J = 6.0$ Hz, 2H), 2.33–2.30 (m, 2H); ESI-MS m/z : 389.0 $[M + H]^+$.

4.1.5.2. 7-(3-Bromopropoxy)-5-methoxy-4H-chromen-4-one (7b). Intermediate **7a** was treated with MeI according to the general procedure to give the desired product **7b** as a yellow solid, yield 62.0%; $^1\text{H NMR}$ (500 MHz, DMSO- d_6) δ 7.60 (d, $J = 6.0$ Hz, 1H), 6.44 (d, $J = 2.0$ Hz, 1H), 6.36 (d, $J = 2.0$ Hz, 1H), 6.18 (d, $J = 6.0$ Hz, 1H), 4.18 (t, $J = 5.5$ Hz, 2H), 3.94 (s, 3H), 3.62 (t, $J = 6.5$ Hz, 2H), 2.38–2.34 (m, 2H); ESI-MS m/z : 313.0 $[M + H]^+$.

4.1.6. 2-(4-Aminophenyl)-7-(3-bromopropoxy)-4H-chromen-4-one (4l)

A mixture of **4k** (0.1 g, 0.25 mmol), SnCl_2 (0.3 mg, 1.5 mmol), and EtOH (7 mL) was stirred under reflux for 1 h. After the mixture was cooled to room temperature, NaOH (1 M, 50 mL) was added until the mixture became alkaline. After extraction with ethyl acetate, the combined organic layers were washed with brine, dried over anhydrous Na_2SO_4 , and evaporated to give **4l** as a yellow solid, yield 92.0%; $^1\text{H NMR}$ (500 MHz, $\text{CDCl}_3 + \text{CD}_3\text{OD}$) δ 7.77 (dd, $J = 7.0$, 2.0 Hz, 2H), 7.36 (d, $J = 2.5$ Hz, 1H), 7.00 (d, $J = 2.5$ Hz, 1H), 6.80 (dd, $J = 7.0$, 2.0 Hz, 2H), 6.65 (s, 1H), 4.26 (t, $J = 6.0$ Hz, 2H), 3.65 (t, $J = 6.0$ Hz, 2H), 2.43–2.38 (m, 2H); ESI-MS m/z : 374.0 $[M + H]^+$.

4.1.7. 7-(3-Bromopropoxy)-2-(4-(dimethylamino)phenyl)-4H-chromen-4-one (4m)

To a stirred mixture of **4l** (90.0 mg, 0.24 mmol) and para-formaldehyde (71.0 mg, 2.4 mmol) in AcOH (10 mL) was added NaCNBH_3 (74.5 mg, 1.2 mmol) in one portion at room temperature. The resulting mixture was stirred at room temperature for 3 h, and NaOH (1 M, 50 mL) was added followed by extraction with CH_2Cl_2 . The organic phase was dried over anhydrous Na_2SO_4 . The solvent was removed, and the residue was purified by silica gel chromatography with hexane/ethyl acetate (4:1) to give **4m** as a yellow solid, yield 81.3%; $^1\text{H NMR}$ (500 MHz, CDCl_3) δ 8.12–8.10 (m, 1H), 7.79 (dt, $J = 8.5$, 3.0 Hz, 2H), 6.95–6.93 (m, 2H), 6.75 (dt, $J = 9.0$, 3.0 Hz, 2H), 6.64 (s, 1H), 4.23 (t, $J = 6.0$ Hz, 2H), 3.63 (t, $J = 6.5$ Hz, 2H), 3.06 (s, 6H), 2.41–2.36 (m, 2H); ESI-MS m/z : 402.1 $[M + H]^+$.

4.1.8. General procedures for the preparation of intermediate **10a** and **10b**

A mixture of **9** (10 mmol) and aminoethanol or 3-amino-1-propano (60 mmol) was heated to 160 °C for 8 h. When the reaction was completed, it was diluted with CH_2Cl_2 , washed with water, followed by brine solution. The organic layer was dried over anhydrous Na_2SO_4 and concentrated under reduced pressure. The obtained residue was purified by silica gel chromatography with $\text{CH}_2\text{Cl}_2/\text{MeOH}$ (20:1) as eluent to give compounds **10a** and **10b** as pale white solid.

4.1.8.1. 2-((1,2,3,4-Tetrahydroacridin-9-yl)amino)ethanol (10a). Intermediate **9** was treated with aminoethanol according to the general procedure to give the desired product **10a** as a pale white solid, yield 81.0%; $^1\text{H NMR}$ (500 MHz, CDCl_3) δ 8.00 (d, $J = 8.5$ Hz, 1H), 7.94 (d, $J = 8.5$ Hz, 1H), 7.56 (t, $J = 7.5$ Hz, 1H), 7.36 (t, $J = 6.0$ Hz, 1H), 3.84 (t, $J = 5.5$ Hz, 2H), 3.64 (br s, 2H), 3.07 (d, $J = 6.0$ Hz, 2H), 2.77 (br s, 2H), 1.91 (t, $J = 3.5$ Hz, 4H); ESI-MS m/z : 243.1 $[M + H]^+$.

4.1.8.2. 3-((1,2,3,4-Tetrahydroacridin-9-yl)amino)propan-1-ol (10b). Intermediate **9** was treated with 3-amino-1-propano according to the general procedure to give the desired product **10b** as a pale white solid, yield 78.5%; $^1\text{H NMR}$ (500 MHz, CDCl_3) δ 8.02 (d,

$J = 8.5$ Hz, 1H), 7.95 (d, $J = 8.5$ Hz, 1H), 7.56 (t, $J = 6.5$ Hz, 1H), 7.34 (t, $J = 6.5$ Hz, 1H), 3.94 (t, $J = 5.5$ Hz, 2H), 3.72 (t, $J = 5.5$ Hz, 2H), 3.05 (d, $J = 6.0$ Hz, 2H), 2.71 (d, $J = 5.5$ Hz, 2H), 2.00–1.95 (m, 2H), 1.90–1.88 (m, 4H); ESI-MS m/z : 257.1 [M + H]⁺.

4.1.9. General procedures for the preparation of intermediate **12a** and **12b**

To a solution of **10** (5.0 mmol) and Et₃N (6.0 mmol) in CH₂Cl₂ (10 mL) was drop wise added *p*-methyl benzene sulfonic chloride (5.5 mmol) in CH₂Cl₂ (10 mL) at 0 °C. The mixture was stirred for 2 h at room temperature. When the reaction was completed, it was diluted with CH₂Cl₂, washed with water, followed by brine solution. The organic layer was dried over anhydrous Na₂SO₄ and concentrated under reduced pressure. The crude product **11** was dissolved in DMF (40 mL) without purification. Anhydrous piperazine (40 mmol) was added and stirred at 80 °C for 2 h. After cooling, the solvent was dissolved in CH₂Cl₂ (40 mL) and then washed with water (30 mL × 3). The organic phase was dried over anhydrous Na₂SO₄ and concentrated under reduced pressure. The crude product was purified by silica gel chromatography with CH₂Cl₂/MeOH (20:1) as eluent to afford compound **12** as yellow oil.

4.1.9.1. N-(2-(Piperazin-1-yl)ethyl)-1,2,3,4-tetrahydroacridin-9-amine (12a). Intermediate **10a** was treated with *p*-methyl benzene sulfonic chloride to afford **11a** followed by piperazine according to the general procedure to give the desired product **12a** as yellow oil, yield 58.5%; ¹H NMR (500 MHz, CDCl₃) δ 8.06 (d, $J = 8.5$ Hz, 2H), 7.59 (t, $J = 7.0$ Hz, 1H), 7.36 (t, $J = 8.0$ Hz, 1H), 3.65 (br s, 2H), 3.14 (br s, 2H), 2.95 (t, $J = 5.0$ Hz, 2H), 2.74 (br s, 2H), 2.63 (t, $J = 6.0$ Hz, 4H), 2.53–2.51 (m, 4H), 1.92–1.90 (m, 4H); ESI-MS m/z : 311.2 [M + H]⁺.

4.1.9.2. N-(3-(Piperazin-1-yl)propyl)-1,2,3,4-tetrahydroacridin-9-amine (12b). Intermediate **10b** was treated with *p*-methyl benzene sulfonic chloride to afford **11b** followed by piperazine according to the general procedure to give the desired product **12b** as yellow oil, yield 50.6%; ¹H NMR (500 MHz, CDCl₃) δ 8.05 (d, $J = 8.5$ Hz, 1H), 8.00 (d, $J = 8.5$ Hz, 1H), 7.56 (t, $J = 7.0$ Hz, 1H), 7.34 (t, $J = 7.0$ Hz, 1H), 3.66 (t, $J = 6.0$ Hz, 2H), 3.10 (br s, 2H), 3.00–2.88 (m, 6H), 2.59–2.50 (m, 6H), 1.92 (t, $J = 3.0$ Hz, 4H), 1.89–1.85 (m, 2H); ESI-MS m/z : 325.2 [M + H]⁺.

4.1.10. General procedures for the preparation of compounds **13a–u**

A mixture of **12a–b** (2.5 mmol), anhydrous K₂CO₃ (2.5 mmol) and the corresponding flavonoid derivatives **4a–m** or **7a–c** (2.5 mmol) in dry acetonitrile was refluxed for 8 h. After cooling to the room temperature, the mixture was filtered and the filtrate was evaporated under vacuum. The obtained residue was purified by silica gel chromatography with CH₂Cl₂/MeOH (15:1) as eluent to yield target compounds **13a–u**.

4.1.10.1. 2-Phenyl-7-(2-(4-(2-((1,2,3,4-tetrahydroacridin-9-yl)amino)ethyl)piperazin-1-yl)ethoxy)-4H-chromen-4-one (13a). Intermediate **12a** was treated with **4a** according to the general procedure to give the desired product **13a** as a pale white solid, yield 48.5%, m.p. 89–93 °C; IR (KBr) ν 3424, 2935, 2814, 1636, 1602, 1499, 1447, 1375, 1260, 1163, 1088, 773, 676 cm⁻¹; ¹H NMR (500 MHz, CDCl₃): δ 8.14 (d, $J = 8.5$ Hz, 1H), 8.10 (d, $J = 9.0$ Hz, 1H), 7.90 (dd, $J = 7.5, 2.0$ Hz, 2H), 7.65 (t, $J = 7.5$ Hz, 1H), 7.56–7.50 (m, 3H), 7.40 (t, $J = 7.5$ Hz, 1H), 7.02–7.00 (m, 2H), 6.77 (s, 1H), 4.25 (t, $J = 5.5$ Hz, 2H), 3.81 (br s, 2H), 3.23 (br s, 2H), 2.92 (t, $J = 5.5$ Hz, 2H), 2.72–2.63 (m, 12H), 1.93–1.92 (m, 4H); ¹³C NMR (125 MHz, CDCl₃): δ 177.8, 163.3, 163.1, 158.0, 155.8, 151.7, 139.0, 132.1, 131.9, 131.5, 129.1, 127.2, 126.2, 124.5, 123.4, 121.8, 118.1, 115.5, 114.6, 107.7, 101.3, 66.9, 56.9, 56.7, 53.9, 52.4, 44.2, 29.1, 24.0, 22.5, 21.6; ESI-MS m/z :

575.3 [M + H]⁺; HRMS: calcd for C₃₆H₃₉N₄O₃ [M + H]⁺, 575.3017, found 575.3015.

4.1.10.2. 2-Phenyl-7-(3-(4-(2-((1,2,3,4-tetrahydroacridin-9-yl)amino)ethyl)piperazin-1-yl)propoxy)-4H-chromen-4-one (13b). Intermediate **12a** was treated with **4b** according to the general procedure to give the desired product **13b** as a pale white solid, yield 50.4%, m.p. 76–78 °C; IR (KBr) ν 3345, 2935, 2812, 1640, 1569, 1498, 1447, 1374, 1162, 1088, 769, 681 cm⁻¹; ¹H NMR (500 MHz, CDCl₃): δ 8.14 (dd, $J = 6.0, 3.0$ Hz, 1H), 8.05–8.00 (m, 2H), 7.92–7.90 (m, 2H), 7.57 (t, $J = 7.5$ Hz, 1H), 7.53–7.50 (m, 3H), 7.35 (t, $J = 7.5$ Hz, 1H), 7.00–6.99 (m, 2H), 6.77 (s, 1H), 4.17 (t, $J = 6.0$ Hz, 2H), 3.62 (br s, 2H), 3.11 (br s, 2H), 2.75 (br s, 2H), 2.64 (t, $J = 5.5$ Hz, 2H), 2.61–2.58 (m, 8H), 2.08–2.03 (m, 4H), 1.93 (t, $J = 3.5$ Hz, 4H); ¹³C NMR (125 MHz, CDCl₃): δ 178.3, 164.1, 163.5, 158.5, 155.9, 151.5, 138.9, 132.4, 132.0, 131.8, 129.5, 127.8, 126.6, 124.2, 123.4, 121.1, 118.3, 115.1, 110.1, 108.1, 115.1, 110.1, 108.1, 101.5, 100.4, 67.3, 57.8, 55.3, 54.0, 53.1, 45.4, 30.1, 27.0, 25.2, 23.4, 23.0; ESI-MS m/z : 589.3 [M + H]⁺; HRMS: calcd for C₃₇H₄₁N₄O₃ [M + H]⁺, 589.3173, found 589.3170.

4.1.10.3. 2-Phenyl-7-(4-(4-(2-((1,2,3,4-tetrahydroacridin-9-yl)amino)ethyl)piperazin-1-yl)butoxy)-4H-chromen-4-one (13c). Intermediate **12a** was treated with **4c** according to the general procedure to give the desired product **13c** as a pale white solid, yield 52.3%, m.p. 75–77 °C; IR (KBr) ν 3347, 3056, 2932, 2810, 1639, 1603, 1499, 1447, 1374, 1248, 1161, 1088, 769, 689 cm⁻¹; ¹H NMR (500 MHz, CDCl₃): δ 8.13 (d, $J = 8.5$ Hz, 2H), 8.07 (d, $J = 8.5$ Hz, 1H), 7.91–7.89 (m, 2H), 7.60 (t, $J = 7.5$ Hz, 1H), 7.55–7.50 (m, 3H), 7.37 (t, $J = 8.0$ Hz, 1H), 6.99–6.96 (m, 2H), 6.76 (s, 1H), 4.12 (t, $J = 6.0$ Hz, 2H), 3.69 (br s, 2H), 3.16 (br s, 2H), 2.71 (br s, 2H), 2.66 (t, $J = 5.5$ Hz, 2H), 2.64–2.48 (m, 6H), 2.47 (t, $J = 7.5$ Hz, 4H), 1.93–1.89 (m, 6H), 1.76–1.74 (m, 2H); ¹³C NMR (125 MHz, CDCl₃): δ 178.0, 163.8, 163.2, 158.1, 156.1, 149.7, 138.9, 132.1, 131.6, 129.2, 127.2, 126.3, 123.3, 118.0, 114.8, 107.8, 101.2, 68.6, 58.2, 57.2, 53.6, 52.8, 44.8, 32.1, 29.8, 27.1, 24.5, 23.6, 22.9, 22.3; ESI-MS m/z : 603.3 [M + H]⁺; HRMS: calcd for C₃₈H₄₃N₄O₃ [M + H]⁺, 603.3330, found 603.3327.

4.1.10.4. 2-Phenyl-7-((5-(4-(2-((1,2,3,4-tetrahydroacridin-9-yl)amino)ethyl)piperazin-1-yl)pentyl)oxy)-4H-chromen-4-one (13d). Intermediate **12a** was treated with **4d** according to the general procedure to give the desired product **13d** as a pale white solid, yield 50.5%, m.p. 86–88 °C; IR (KBr) ν 3419, 2931, 2811, 2353, 1641, 1602, 1518, 1447, 1374, 1248, 1161, 1087, 772, 676 cm⁻¹; ¹H NMR (500 MHz, CDCl₃): δ 8.27 (d, $J = 5.5$ Hz, 1H), 8.13 (d, $J = 9.0$ Hz, 1H), 8.09 (d, $J = 8.5$ Hz, 1H), 7.92–7.90 (m, 2H), 7.64 (t, $J = 8.0$ Hz, 1H), 7.55–7.50 (m, 3H), 7.39 (t, $J = 8.0$ Hz, 1H), 6.99–6.95 (m, 2H), 6.77 (s, 1H), 4.10 (t, $J = 6.0$ Hz, 2H), 3.79–3.74 (m, 2H), 3.24–3.23 (m, 2H), 2.70 (t, $J = 5.5$ Hz, 2H), 2.69–2.66 (m, 2H), 2.65–2.45 (m, 6H), 2.45 (t, $J = 7.5$ Hz, 2H), 2.07 (br s, 2H), 1.93–1.86 (m, 6H), 1.66–1.61 (m, 2H), 1.59–1.55 (m, 2H); ¹³C NMR (125 MHz, CDCl₃): δ 177.9, 163.7, 163.1, 158.1, 155.9, 152.2, 139.5, 132.0, 131.9, 131.4, 129.0, 127.1, 126.2, 124.4, 123.3, 117.8, 115.7, 114.7, 110.2, 107.6, 101.0, 68.5, 58.4, 56.8, 53.4, 52.4, 44.3, 31.9, 28.9, 26.5, 24.0, 22.5, 21.9, 21.7; ESI-MS m/z : 617.3 [M + H]⁺; HRMS: calcd for C₃₉H₄₅N₄O₃ [M + H]⁺, 617.3486, found 617.3488.

4.1.10.5. 2-Phenyl-7-((6-(4-(2-((1,2,3,4-tetrahydroacridin-9-yl)amino)ethyl)piperazin-1-yl)hexyl)oxy)-4H-chromen-4-one (13e). Intermediate **12a** was treated with **4e** according to the general procedure to give the desired product **13e** as a pale white solid, yield 48.5%, m.p. 88–90 °C; IR (KBr) ν 3398, 3064, 2934, 2809, 2313, 1640, 1603, 1498, 1374, 1248, 1161, 1088, 771, 689 cm⁻¹; ¹H NMR (500 MHz, CDCl₃): δ 8.50 (br s, 1H), 8.13 (d, $J = 8.5$ Hz, 2H), 7.92–7.90 (m, 2H), 7.68 (t, $J = 8.0$ Hz, 1H), 7.53–7.51 (m, 3H), 7.42 (t, $J = 7.5$ Hz, 1H), 6.99–6.96 (m, 2H), 6.77 (s, 1H), 4.09 (t, $J = 6.0$ Hz,

2H), 3.88 (br s, 2H), 3.31 (br s, 2H), 2.62–2.45 (m, 8H), 2.40 (t, $J = 7.5$ Hz, 2H), 1.96–1.90 (m, 4H), 1.90–1.85 (m, 2H), 1.60–1.51 (m, 6H), 1.46–1.40 (m, 2H); ^{13}C NMR (125 MHz, CDCl_3): δ 177.8, 163.7, 163.0, 158.1, 139.6, 132.2, 132.0, 131.4, 129.0, 127.1, 126.2, 125.0, 123.6, 121.2, 117.8, 115.2, 114.7, 109.7, 107.6, 101.0, 68.6, 58.5, 56.3, 53.6, 52.4, 49.0, 29.0, 27.2, 26.9, 26.0, 25.4, 23.7, 22.1, 21.1; ESI-MS m/z : 631.4 $[\text{M} + \text{H}]^+$; HRMS: calcd for $\text{C}_{40}\text{H}_{47}\text{N}_4\text{O}_3$ $[\text{M} + \text{H}]^+$, 631.3643, found 631.3647.

4.1.10.6. 2-Phenyl-7-(2-(4-(3-((1,2,3,4-tetrahydroacridin-9-yl)amino)propyl)piperazin-1-yl)ethoxy)-4H-chromen-4-one (**13f**).

Intermediate **12b** was treated with **4a** according to the general procedure to give the desired product **13f** as a pale white solid, yield 53.0%, m.p. 128–130 °C; IR (KBr) ν 3398, 3056, 2934, 2812, 2320, 1631, 1597, 1523, 1447, 1375, 1249, 1164, 1088, 775, 676 cm^{-1} ; ^1H NMR (500 MHz, CDCl_3): δ 8.62 (d, $J = 8.5$ Hz, 1H), 8.24 (d, $J = 9.0$ Hz, 1H), 8.14 (d, $J = 9.0$ Hz, 1H), 7.91 (dd, $J = 7.5, 2.5$ Hz, 2H), 7.69 (t, $J = 8.0$ Hz, 1H), 7.56–7.54 (m, 3H), 7.42 (t, $J = 7.5$ Hz, 1H), 7.05–6.97 (m, 2H), 6.77 (s, 1H), 4.25 (d, $J = 5.0$ Hz, 2H), 4.14 (d, $J = 5.0$ Hz, 2H), 3.36 (t, $J = 6.0$ Hz, 2H), 2.96–2.92 (m, 2H), 2.83–2.65 (m, 8H), 2.62 (d, $J = 6.5$ Hz, 2H), 2.06–2.00 (m, 2H), 1.94 (d, $J = 5.0$ Hz, 2H), 1.88 (t, $J = 5.0$ Hz, 2H), 1.73–1.59 (m, 2H); ^{13}C NMR (125 MHz, CDCl_3): δ 177.7, 163.2, 162.7, 158.0, 155.8, 151.3, 151.2, 139.0, 132.3, 131.9, 131.5, 129.1, 127.3, 126.2, 125.0, 124.3, 121.1, 118.2, 115.9, 114.6, 110.7, 107.7, 101.3, 66.8, 57.0, 56.5, 53.7, 52.8, 29.7, 28.4, 25.6, 25.2, 21.8, 20.8; ESI-MS m/z : 589.3 $[\text{M} + \text{H}]^+$; HRMS: calcd for $\text{C}_{37}\text{H}_{41}\text{N}_4\text{O}_3$ $[\text{M} + \text{H}]^+$, 589.3173, found 589.3176.

4.1.10.7. 2-Phenyl-7-(3-(4-(3-((1,2,3,4-tetrahydroacridin-9-yl)amino)propyl)piperazin-1-yl)propoxy)-4H-chromen-4-one (**13g**).

Intermediate **12b** was treated with **4b** according to the general procedure to give the desired product **13g** as a pale white solid, yield 46.5%, m.p. 99–101 °C; IR (KBr) ν 3422, 2936, 2814, 2319, 1634, 1602, 1447, 1375, 1250, 1165, 1088, 771, 677 cm^{-1} ; ^1H NMR (500 MHz, CDCl_3): δ 8.41 (br s, 1H), 8.17–8.13 (m, 2H), 7.92–7.90 (m, 2H), 7.66 (t, $J = 7.5$ Hz, 1H), 7.55–7.51 (m, 3H), 7.39 (t, $J = 8.0$ Hz, 1H), 7.01–6.99 (m, 2H), 6.77 (s, 1H), 4.18 (t, $J = 6.0$ Hz, 2H), 3.94 (br s, 2H), 3.28 (br s, 2H), 2.66 (m, 6H), 2.61–2.58 (m, 6H), 2.09–2.04 (m, 2H), 1.96–1.90 (m, 6H), 1.60 (br s, 2H); ^{13}C NMR (125 MHz, CDCl_3): δ 177.8, 163.6, 163.1, 158.0, 154.5, 154.4, 131.9, 131.5, 131.0, 129.0, 128.4, 127.1, 126.2, 124.4, 124.0, 123.3, 117.9, 117.1, 114.7, 112.2, 107.6, 101.1, 66.8, 58.3, 54.9, 54.0, 52.9, 50.0, 29.9, 29.7, 26.6, 25.8, 25.7, 22.1, 21.4; ESI-MS m/z : 603.3 $[\text{M} + \text{H}]^+$; HRMS: calcd for $\text{C}_{38}\text{H}_{43}\text{N}_4\text{O}_3$ $[\text{M} + \text{H}]^+$, 603.3330, found 603.3331.

4.1.10.8. 2-Phenyl-7-(4-(4-(3-((1,2,3,4-tetrahydroacridin-9-yl)amino)propyl)piperazin-1-yl)butoxy)-4H-chromen-4-one (**13h**).

Intermediate **12b** was treated with **4c** according to the general procedure to give the desired product **13h** as a pale white solid, yield 50.2%, m.p. 165–166 °C; IR (KBr) ν 3422, 3239, 2933, 2812, 2320, 1633, 1597, 1518, 1448, 1356, 1244, 1085, 785, 750 cm^{-1} ; ^1H NMR (500 MHz, CDCl_3): δ 8.61 (d, $J = 8.5$ Hz, 1H), 8.23 (d, $J = 8.5$ Hz, 1H), 8.13 (d, $J = 8.5$ Hz, 1H), 7.91–7.89 (m, 2H), 7.68 (t, $J = 8.0$ Hz, 1H), 7.54–7.51 (m, 3H), 7.41 (t, $J = 8.0$ Hz, 1H), 6.99–6.96 (m, 2H), 6.76 (s, 1H), 4.15–4.12 (m, 4H), 3.45 (t, $J = 5.5$ Hz, 2H), 2.73 (m, 6H), 2.62–2.60 (m, 6H), 2.51 (br s, 2H), 1.98 (br s, 2H), 1.96–1.88 (m, 6H), 1.77 (br s, 2H); ^{13}C NMR (125 MHz, CDCl_3): δ 177.8, 163.6, 163.0, 159.0, 155.8, 151.2, 139.1, 131.5, 129.1, 127.1, 126.2, 124.4, 121.0, 117.9, 115.9, 114.7, 110.9, 107.6, 101.1, 68.3, 58.1, 53.8, 52.6, 50.1, 28.4, 26.9, 25.7, 25.2, 23.3, 21.8, 20.8; ESI-MS m/z : 617.3 $[\text{M} + \text{H}]^+$; HRMS: calcd for $\text{C}_{39}\text{H}_{45}\text{N}_4\text{O}_3$ $[\text{M} + \text{H}]^+$, 617.3486, found 617.3489.

4.1.10.9. 2-Phenyl-7-((5-(4-(3-((1,2,3,4-tetrahydroacridin-9-yl)amino)propyl)piperazin-1-yl)pentyl)oxy)-4H-chromen-4-one (**13i**).

Intermediate **12b** was treated with **4d** according to the general

procedure to give the desired product **13i** as a pale white solid, yield 49.2%, m.p. 75–78 °C; IR (KBr) ν 3420, 2934, 2810, 1639, 1602, 1499, 1446, 1373, 1248, 1159, 1087, 771, 680 cm^{-1} ; ^1H NMR (500 MHz, CDCl_3): δ 8.29 (br s, 1H), 8.13 (d, $J = 9.0$ Hz, 2H), 7.92–7.90 (m, 2H), 7.63 (m, 1H), 7.53–7.50 (m, 3H), 7.37 (t, $J = 7.5$ Hz, 1H), 6.99–6.96 (m, 2H), 6.77 (s, 1H), 4.10 (t, $J = 6.0$ Hz, 2H), 3.85 (br s, 2H), 3.23 (br s, 2H), 2.67–2.63 (m, 6H), 2.60–2.52 (m, 4H), 2.42 (t, $J = 7.5$ Hz, 2H), 1.92–1.87 (m, 8H), 1.65–1.55 (m, 6H); ^{13}C NMR (125 MHz, CDCl_3): δ 177.8, 163.7, 163.0, 158.0, 155.7, 152.0, 138.2, 132.3, 132.0, 131.4, 129.0, 127.1, 126.2, 124.2, 123.7, 121.2, 117.8, 115.8, 114.7, 111.6, 107.6, 101.0, 68.6, 58.6, 58.2, 53.9, 49.9, 31.0, 28.9, 26.6, 26.2, 25.7, 24.0, 22.4, 21.9; ESI-MS m/z : 631.3 $[\text{M} + \text{H}]^+$; HRMS: calcd for $\text{C}_{40}\text{H}_{47}\text{N}_4\text{O}_3$ $[\text{M} + \text{H}]^+$, 631.3643, found 631.3644.

4.1.10.10. 2-Phenyl-7-((6-(4-(3-((1,2,3,4-tetrahydroacridin-9-yl)amino)propyl)piperazin-1-yl)hexyl)oxy)-4H-chromen-4-one (**13j**).

Intermediate **12b** was treated with **4e** according to the general procedure to give the desired product **13j** as a pale white solid, yield 52.0%, m.p. 104–106 °C; IR (KBr) ν 3422, 2932, 2311, 1632, 1601, 1524, 1447, 1374, 1355, 1247, 1166, 1087, 772, 678 cm^{-1} ; ^1H NMR (500 MHz, CDCl_3): δ 8.62 (d, $J = 8.0$ Hz, 1H), 8.23 (d, $J = 8.5$ Hz, 1H), 8.13 (d, $J = 8.5$ Hz, 1H), 7.92–7.90 (m, 2H), 7.69 (t, $J = 7.5$ Hz, 1H), 7.53–7.50 (m, 3H), 7.42 (t, $J = 7.0$ Hz, 1H), 7.00–6.96 (m, 2H), 6.76 (s, 1H), 4.12–4.08 (m, 4H), 3.52 (br s, 2H), 2.75–2.74 (m, 6H), 2.61–2.57 (m, 4H), 2.45 (br s, 2H), 1.98–1.93 (m, 4H), 1.89–1.85 (m, 4H), 1.60–1.52 (m, 6H), 1.48–1.43 (m, 2H); ^{13}C NMR (125 MHz, CDCl_3): δ 177.8, 163.7, 163.1, 158.1, 155.8, 151.2, 139.1, 132.2, 131.9, 131.4, 129.1, 127.1, 126.2, 124.9, 124.4, 121.1, 117.8, 115.9, 114.7, 107.6, 101.0, 68.6, 58.5, 53.6, 52.5, 49.9, 29.7, 28.9, 28.4, 27.1, 25.6, 25.4, 21.8, 20.8; ESI-MS m/z : 645.4 $[\text{M} + \text{H}]^+$; HRMS: calcd for $\text{C}_{41}\text{H}_{49}\text{N}_4\text{O}_3$ $[\text{M} + \text{H}]^+$, 645.3799, found 645.3805.

4.1.10.11. 5-Hydroxy-2-phenyl-7-(3-(4-(3-((1,2,3,4-tetrahydroacridin-9-yl)amino)propyl)piperazin-1-yl)propoxy)-4H-chromen-4-one (**13k**).

Intermediate **12b** was treated with **4f** according to the general procedure to give the desired product **13k** as a light yellow solid, yield 45.0%, m.p. 84–86 °C; IR (KBr) ν 3423, 2932, 2815, 2320, 1659, 1614, 1586, 1502, 1450, 1351, 1167, 767, 678 cm^{-1} ; ^1H NMR (500 MHz, CDCl_3): δ 12.72 (s, 1H), 8.28 (br s, 1H), 8.13 (d, $J = 8.0$ Hz, 1H), 7.89–7.88 (m, 2H), 7.63 (t, $J = 7.0$ Hz, 1H), 7.57–7.48 (m, 3H), 7.37 (t, $J = 7.5$ Hz, 1H), 6.67 (s, 1H), 6.51 (d, $J = 2.0$ Hz, 1H), 6.38 (d, $J = 2.0$ Hz, 1H), 4.15–4.10 (m, 2H), 3.86 (br s, 2H), 3.22 (br s, 2H), 2.67–2.64 (m, 6H), 2.58–2.55 (m, 6H), 2.05–2.00 (m, 2H), 1.93–1.92 (m, 6H), 1.26 (t, $J = 7.5$ Hz, 2H); ^{13}C NMR (125 MHz, CDCl_3): δ 182.5, 165.1, 164.0, 162.3, 157.9, 156.1, 132.9, 131.8, 131.4, 129.1, 126.3, 124.2, 123.7, 105.9, 105.7, 98.6, 93.3, 66.8, 60.4, 58.2, 54.9, 53.9, 53.0, 49.8, 29.7, 26.6, 25.7, 22.4, 21.8; ESI-MS m/z : 619.3 $[\text{M} + \text{H}]^+$; HRMS: calcd for $\text{C}_{38}\text{H}_{43}\text{N}_4\text{O}_4$ $[\text{M} + \text{H}]^+$, 619.3279, found 619.3282.

4.1.10.12. 5-Methoxy-2-phenyl-7-(3-(4-(3-((1,2,3,4-tetrahydroacridin-9-yl)amino)propyl)piperazin-1-yl)propoxy)-4H-chromen-4-one (**13l**).

Intermediate **12b** was treated with **4g** according to the general procedure to give the desired product **13l** as a light yellow solid, yield 45.2%, m.p. 113–115 °C; IR (KBr) ν 3423, 2931, 2814, 2311, 1643, 1605, 1523, 1449, 1348, 1164, 1118, 767, 693 cm^{-1} ; ^1H NMR (500 MHz, CDCl_3): δ 8.48 (br s, 1H), 8.25 (d, $J = 8.5$ Hz, 1H), 7.88–7.86 (m, 2H), 7.65 (t, $J = 7.0$ Hz, 1H), 7.53–7.47 (m, 3H), 7.41 (t, $J = 8.0$ Hz, 1H), 6.68 (s, 1H), 6.58 (s, 1H), 6.38 (d, $J = 2.0$ Hz, 1H), 4.16–4.10 (m, 4H), 3.96 (s, 3H), 3.28 (br s, 2H), 2.88–2.75 (m, 6H), 2.69–2.61 (m, 6H), 1.91–1.86 (m, 4H), 1.60–1.56 (m, 4H), 1.26 (t, $J = 7.0$ Hz, 2H); ^{13}C NMR (125 MHz, CDCl_3): δ 177.8, 163.4, 163.3, 157.9, 155.8, 151.2, 142.1, 132.3, 131.6, 129.7, 129.1, 127.0, 126.1, 125.1, 124.4, 120.8, 118.0, 115.8, 114.5, 111.0, 107.0, 101.2, 66.5, 58.0, 54.7, 28.4, 26.3, 25.5, 21.8, 21.5, 20.7; ESI-MS m/z : 633.3

[M + H]⁺; HRMS: calcd for C₃₉H₄₅N₄O₄ [M + H]⁺, 633.3435, found 633.3437.

4.1.10.13. 7-(3-(4-(3-((1,2,3,4-Tetrahydroacridin-9-yl)amino)propyl)piperazin-1-yl)propoxy)-2-(p-tolyl)-4H-chromen-4-one (**13m**). Intermediate **12b** was treated with **4h** according to the general procedure to give the desired product **13m** as a pale white solid, yield 46.5%, m.p. 121–124 °C; IR (KBr) ν 3425, 2937, 2815, 2309, 1629, 1597, 1521, 1441, 1373, 1251, 1167, 1088, 822, 760 cm⁻¹; ¹H NMR (500 MHz, CDCl₃): δ 8.51 (d, *J* = 8.5 Hz, 1H), 8.23 (d, *J* = 8.5 Hz, 1H), 8.10–8.08 (m, 1H), 7.77 (d, *J* = 8.5 Hz, 2H), 7.63 (t, *J* = 7.5 Hz, 1H), 7.38 (t, *J* = 7.5 Hz, 1H), 7.29 (d, *J* = 8.0 Hz, 2H), 6.95–6.93 (m, 2H), 6.70 (s, 1H), 4.16–4.09 (m, 4H), 3.27 (br s, 2H), 2.90–2.70 (m, 6H), 2.65–2.59 (m, 6H), 2.41 (s, 3H), 2.08 (br s, 4H), 1.90–1.84 (m, 4H), 1.23 (t, *J* = 7.0 Hz, 2H); ¹³C NMR (125 MHz, CDCl₃): δ 177.5, 161.0, 160.7, 159.9, 155.8, 151.4, 132.25, 131.6, 131.2, 128.9, 127.4, 126.0, 125.3, 124.2, 115.9, 109.2, 96.5, 93.5, 66.2, 60.4, 56.5, 52.9, 46.6, 29.7, 29.7, 28.4, 25.6, 25.2, 21.9, 20.7; ESI-MS *m/z*: 617.3 [M + H]⁺; HRMS: calcd for C₃₉H₄₅N₄O₃ [M + H]⁺, 617.3486, found 617.3484.

4.1.10.14. 2-(4-Methoxyphenyl)-7-(3-(4-(3-((1,2,3,4-tetrahydroacridin-9-yl)amino)propyl)piperazin-1-yl)propoxy)-4H-chromen-4-one (**13n**). Intermediate **12b** was treated with **4i** according to the general procedure to give the desired product **13n** as a pale white solid, yield 50.5%, m.p. 79–81 °C; IR (KBr) ν 3420, 2928, 2814, 2311, 1629, 1604, 1510, 1441, 1374, 1256, 1179, 1088, 830, 760 cm⁻¹; ¹H NMR (500 MHz, DMSO-*d*₆): δ 8.28 (d, *J* = 8.5 Hz, 1H), 8.04 (d, *J* = 9.0 Hz, 2H), 7.91 (d, *J* = 9.0 Hz, 1H), 7.76 (d, *J* = 8.5 Hz, 1H), 7.69 (t, *J* = 7.0 Hz, 1H), 7.44 (t, *J* = 8.0 Hz, 1H), 7.28 (d, *J* = 2.5 Hz, 1H), 7.11 (d, *J* = 8.5 Hz, 2H), 7.02 (dd, *J* = 8.5, 2.0 Hz, 1H), 6.85 (s, 1H), 4.17 (t, *J* = 6.0 Hz, 2H), 3.86 (s, 3H), 3.73–3.72 (m, 2H), 2.94 (br s, 2H), 2.67 (br s, 2H), 2.51–2.50 (m, 4H), 2.46–2.41 (m, 8H), 1.95–1.90 (m, 2H), 1.83–1.79 (m, 6H); ¹³C NMR (125 MHz, DMSO-*d*₆): δ 177.2, 164.0, 163.2, 162.9, 158.3, 154.9, 154.0, 139.8, 131.1, 128.9, 127.0, 125.2, 124.8, 124.3, 118.7, 117.9, 115.7, 115.4, 114.2, 106.2, 102.3, 67.7, 56.8, 56.4, 55.1, 53.9, 53.5, 47.9, 31.6, 27.4, 26.8, 25.7, 22.9, 22.3; ESI-MS *m/z*: 633.3 [M + H]⁺; HRMS: calcd for C₃₉H₄₅N₄O₄ [M + H]⁺, 633.3435, found 633.3440.

4.1.10.15. 2-(4-Aminophenyl)-7-(3-(4-(3-((1,2,3,4-tetrahydroacridin-9-yl)amino)propyl)piperazin-1-yl)propoxy)-4H-chromen-4-one (**13o**). Intermediate **12b** was treated with **4l** according to the general procedure to give the desired product **13o** as a yellow solid, yield 54.0%, m.p. 96–98 °C; IR (KBr) ν 3422, 2931, 2311, 1625, 1597, 1514, 1442, 1375, 1254, 1183, 832 cm⁻¹; ¹H NMR (500 MHz, CDCl₃ + CD₃OD): δ 8.33 (d, *J* = 9.0 Hz, 1H), 8.06 (d, *J* = 8.5 Hz, 1H), 8.02 (d, *J* = 8.5 Hz, 1H), 7.80–7.76 (m, 1H), 7.75–7.31 (m, 2H), 7.53 (t, *J* = 7.5 Hz, 1H), 7.00–6.97 (m, 2H), 6.77 (d, *J* = 8.5 Hz, 2H), 6.63 (s, 1H), 4.19 (t, *J* = 6.0 Hz, 2H), 4.10 (t, *J* = 6.5 Hz, 2H), 3.11 (t, *J* = 6.0 Hz, 2H), 2.84–2.76 (m, 8H), 2.70–2.67 (m, 4H), 2.12 (br s, 4H), 2.01–1.93 (m, 4H); ¹³C NMR (125 MHz, CDCl₃ + CD₃OD) δ 178.7, 164.8, 163.4, 157.9, 156.3, 150.9, 150.5, 138.6, 132.76, 127.9, 126.6, 125.3, 124.9, 119.9, 119.6, 117.4, 115.8, 114.5, 111.3, 103.8, 101.0, 100.0, 66.5, 54.7, 52.6, 51.9, 28.2, 25.9, 25.6, 24.8, 21.7, 20.6. ESI-MS *m/z*: 618.3 [M + H]⁺; HRMS: calcd for C₄₀H₄₈N₅O₃ [M + H]⁺, 618.3439, found 618.3440.

4.1.10.16. 2-(4-(Dimethylamino)phenyl)-7-(3-(4-(3-((1,2,3,4-tetrahydroacridin-9-yl)amino)propyl)piperazin-1-yl)propoxy)-4H-chromen-4-one (**13p**). Intermediate **12b** was treated with **4m** according to the general procedure to give the desired product **13p** as a yellow solid, yield 49.5%, m.p. 90–92 °C; IR (KBr) ν 3422, 2934, 2810, 2310, 1627, 1602, 1522, 1439, 1361, 1260, 1168, 1088, 815, 729 cm⁻¹; ¹H NMR (500 MHz, CDCl₃): δ 8.17–8.09 (m, 3H), 7.79 (d, *J* = 8.5 Hz, 2H), 7.59 (t, *J* = 7.5 Hz, 1H), 7.36 (t, *J* = 8.0 Hz, 1H), 6.96–

6.94 (m, 2H), 6.75 (d, *J* = 9.0 Hz, 2H), 6.63 (s, 1H), 4.16 (t, *J* = 6.0 Hz, 2H), 3.75 (br s, 2H), 3.17–3.16 (m, 2H), 3.07 (s, 6H), 2.71–2.69 (m, 6H), 2.65–2.57 (m, 8H), 2.08–2.02 (m, 2H), 1.94–1.87 (m, 6H); ¹³C NMR (125 MHz, CDCl₃) δ 177.8, 163.9, 163.2, 157.9, 152.4, 127.6, 126.9, 123.9, 123.4, 118.6, 117.9, 114.0, 111.7, 104.4, 101.1, 100.0, 66.8, 57.9, 55.0, 53.8, 53.1, 49.4, 30.9, 29.7, 26.7, 25.7, 22.7, 22.3; ESI-MS *m/z*: 646.4 [M + H]⁺; HRMS: calcd for C₄₀H₄₈N₅O₃ [M + H]⁺, 646.3752, found 646.3755.

4.1.10.17. 2-(4-Chlorophenyl)-7-(3-(4-(3-((1,2,3,4-tetrahydroacridin-9-yl)amino)propyl)piperazin-1-yl)propoxy)-4H-chromen-4-one (**13q**). Intermediate **12b** was treated with **4j** according to the general procedure to give the desired product **13q** as a light yellow solid, yield 51.0%, m.p. 117–119 °C; IR (KBr) ν 3445, 2926, 2872, 2822, 2311, 1638, 1600, 1490, 1440, 1261, 1088, 1035, 802, 756 cm⁻¹; ¹H NMR (500 MHz, DMSO-*d*₆): δ 8.39 (d, *J* = 8.5 Hz, 1H), 8.18 (d, *J* = 8.5 Hz, 2H), 7.99 (d, *J* = 9.0 Hz, 1H), 7.85–7.80 (m, 2H), 7.70 (d, *J* = 8.5 Hz, 2H), 7.56–7.53 (m, 2H), 7.38 (d, *J* = 2.5 Hz, 1H), 7.11 (dd, *J* = 8.5, 2.0 Hz, 1H), 7.06 (s, 1H), 4.24 (t, *J* = 6.0 Hz, 2H), 3.88 (d, *J* = 4.5 Hz, 2H), 3.01 (br s, 2H), 2.72 (br s, 2H), 2.56–2.55 (m, 6H), 2.55–2.40 (m, 8H), 2.01–1.98 (m, 2H), 1.92–1.87 (m, 6H); ¹³C NMR (125 MHz, DMSO-*d*₆): δ 176.6, 163.6, 161.3, 157.4, 153.0, 138.6, 136.7, 131.9, 130.4, 129.4, 128.3, 126.5, 125.2, 124.7, 117.3, 115.4, 114.4, 112.4, 107.4, 101.7, 67.1, 56.1, 54.4, 53.1, 52.7, 47.3, 29.5, 26.4, 26.1, 24.9, 21.9, 21.1; ESI-MS *m/z*: 637.3 [M + H]⁺; HRMS: calcd for C₃₈H₄₂ClN₄O₃ [M + H]⁺, 637.2940, found 637.2943.

4.1.10.18. 2-(4-Nitrophenyl)-7-(3-(4-(3-((1,2,3,4-tetrahydroacridin-9-yl)amino)propyl)piperazin-1-yl)propoxy)-4H-chromen-4-one (**13r**). Intermediate **12b** was treated with **4k** according to the general procedure to give the desired product **13r** as a dark yellow solid, yield 50.5%, m.p. 146–148 °C; IR (KBr) ν 3420, 2927, 2310, 1633, 1608, 1520, 1443, 1346, 1252, 1088, 852, 759 cm⁻¹; ¹H NMR (500 MHz, CDCl₃ + CD₃OD): δ 8.42–8.39 (m, 2H), 8.29 (d, *J* = 8.5 Hz, 1H), 8.19–8.16 (m, 2H), 8.12 (d, *J* = 8.5 Hz, 1H), 7.96 (d, *J* = 7.5 Hz, 1H), 7.76 (t, *J* = 7.5 Hz, 1H), 7.52–7.49 (m, 1H), 7.10–7.06 (m, 2H), 6.92 (s, 1H), 4.22 (t, *J* = 6.0 Hz, 2H), 4.03 (t, *J* = 6.0 Hz, 2H), 3.01 (t, *J* = 6.5 Hz, 2H), 2.70–2.68 (m, 6H), 2.66–2.64 (m, 8H), 2.14–2.09 (m, 2H), 2.03–1.95 (m, 6H); ¹³C NMR (125 MHz, CDCl₃ + CD₃OD) δ 178.9, 164.7, 161.3, 158.5, 155.8, 152.1, 149.8, 140.6, 137.8, 132.4, 127.6, 127.3, 125.2, 125.1, 124.5, 121.3, 117.7, 116.9, 115.9, 112.4, 109.5, 101.4, 67.3, 57.6, 55.4, 53.6, 53.1, 29.4, 26.6, 26.4, 25.3, 22.2, 21.4. ESI-MS *m/z*: 648.3 [M + H]⁺; HRMS: calcd for C₃₈H₄₂N₅O₅ [M + H]⁺, 648.3180, found 648.3186.

4.1.10.19. 5-Hydroxy-7-(3-(4-(3-((1,2,3,4-tetrahydroacridin-9-yl)amino)propyl)piperazin-1-yl)propoxy)-4H-chromen-4-one (**13s**). Intermediate **12b** was treated with **7a** according to the general procedure to give the desired product **13s** as a light yellow solid, yield 45.2%, m.p. 74–76 °C; IR (KBr) ν 3446, 2926, 2310, 1660, 1569, 1502, 1454, 1262, 1162, 1108, 1034, 803, 759 cm⁻¹; ¹H NMR (500 MHz, CDCl₃): δ 12.56 (s, 1H), 8.29 (d, *J* = 3.5 Hz, 1H), 8.14 (d, *J* = 8.5 Hz, 1H), 7.74 (d, *J* = 6.0 Hz, 1H), 7.62 (t, *J* = 7.5 Hz, 1H), 7.39–7.36 (m, 1H), 6.37 (dd, *J* = 12.0, 2.0 Hz, 2H), 6.20 (d, *J* = 6.0 Hz, 1H), 4.10 (t, *J* = 6.5 Hz, 2H), 3.89 (t, *J* = 5.5 Hz, 2H), 3.24–3.21 (m, 2H), 2.69–2.60 (m, 8H), 2.59–2.50 (m, 6H), 2.04–1.98 (m, 2H), 1.96–1.88 (m, 6H); ¹³C NMR (125 MHz, CDCl₃): δ 181.8, 165.0, 162.4, 158.1, 155.6, 153.7, 130.4, 124.2, 123.9, 111.4, 106.7, 98.6, 93.3, 66.8, 58.1, 54.9, 53.9, 53.0, 49.8, 30.9, 29.7, 26.5, 26.2, 25.7, 22.3, 21.7; ESI-MS *m/z*: 543.3 [M + H]⁺; HRMS: calcd for C₃₂H₃₉N₄O₄ [M + H]⁺, 543.2966, found 543.2971.

4.1.10.20. 5-Methoxy-7-(3-(4-(3-((1,2,3,4-tetrahydroacridin-9-yl)amino)propyl)piperazin-1-yl)propoxy)-4H-chromen-4-one (**13t**). Intermediate **12b** was treated with **7b** according to the general

procedure to give the desired product **13t** as a light yellow solid, yield 47.5%, m.p. 96–99 °C; IR (KBr) ν 3420, 2929, 2310, 1648, 1603, 1521, 1455, 1279, 1159, 1107, 1078, 832, 762 cm^{-1} ; ^1H NMR (500 MHz, CDCl_3) δ 8.54 (d, $J = 8.5$ Hz, 1H), 8.25 (d, $J = 8.5$ Hz, 1H), 7.92–7.77 (m, 1H), 7.66 (ddd, $J = 8.5, 6.5, 1.0$ Hz, 1H), 7.61 (d, $J = 6.0$ Hz, 1H), 7.41 (ddd, $J = 8.5, 6.5, 1.0$ Hz, 1H), 6.45 (d, $J = 2.5$ Hz, 1H), 6.36 (d, $J = 2.5$ Hz, 1H), 6.18 (d, $J = 6.0$ Hz, 1H), 4.12 (t, $J = 6.0$ Hz, 4H), 3.93 (s, 3H), 3.31 (t, $J = 6.5$ Hz, 2H), 2.64–2.56 (m, 4H), 2.63–2.57 (m, 8H), 2.06–2.03 (m, 2H), 2.02–1.86 (m, 6H); ^{13}C NMR (125 MHz, CDCl_3) δ 176.5, 163.4, 161.1, 160.1, 155.6, 152.6, 151.4, 139.5, 131.9, 124.8, 124.5, 121.3, 116.1, 114.8, 110.9, 110.4, 96.5, 93.5, 66.6, 58.3, 56.5, 54.9, 53.9, 52.8, 50.1, 28.7, 26.5, 25.7, 25.4, 21.8, 20.9; ESI-MS m/z : 557.3 $[\text{M} + \text{H}]^+$; HRMS: calcd for $\text{C}_{33}\text{H}_{41}\text{N}_4\text{O}_4$ $[\text{M} + \text{H}]^+$, 557.3122, found 557.3127.

4.1.10.21. 7-(3-(4-(3-((1,2,3,4-Tetrahydroacridin-9-yl)amino)propyl)piperazin-1-yl)propoxy)-4H-chromen-4-one (**13u**).

Intermediate **12b** was treated with **7c** according to the general procedure to give the desired product **13u** as a light yellow solid, yield 45.5%, m.p. 172–175 °C; IR (KBr) ν 3409, 2927, 2810, 2309, 1636, 1590, 1521, 1442, 1264, 1228, 1033, 815, 759 cm^{-1} ; ^1H NMR (500 MHz, CDCl_3) δ 8.51 (d, $J = 8.5$ Hz, 1H), 8.22 (d, $J = 8.5$ Hz, 1H), 8.10 (d, $J = 9.0$ Hz, 1H), 7.78 (d, $J = 6.0$ Hz, 1H), 7.70–7.54 (m, 2H), 7.40 (t, $J = 7.5$ Hz, 1H), 6.97 (dd, $J = 9.0, 2.5$ Hz, 1H), 6.86 (d, $J = 2.0$ Hz, 1H), 6.27 (d, $J = 6.0$ Hz, 1H), 4.14 (t, $J = 6.0$ Hz, 2H), 4.07 (s, 2H), 3.30 (t, $J = 6.0$ Hz, 2H), 2.73–2.65 (m, 4H), 2.64–2.57 (m, 8H), 2.08–2.02 (m, 2H), 1.98–1.89 (m, 6H); ^{13}C NMR (125 MHz, CDCl_3) δ 176.9, 163.5, 158.3, 155.3, 154.9, 151.9, 140.2, 131.7, 127.2, 124.6, 124.4, 121.9, 118.8, 116.4, 112.9, 111.3, 101.1, 66.8, 58.4, 55.0, 54.0, 52.9, 50.2, 29.7, 29.1, 26.6, 25.7, 25.5, 21.9, 21.0; ESI-MS m/z : 527.3 $[\text{M} + \text{H}]^+$; HRMS: calcd for $\text{C}_{32}\text{H}_{39}\text{N}_4\text{O}_3$ $[\text{M} + \text{H}]^+$, 527.3017, found 527.3018.

4.2. In vitro inhibition studies on AChE and BuChE

Acetylcholinesterase (AChE, E.C. 3.1.1.7, from electric eel), butyrylcholinesterase (BuChE, E.C. 3.1.1.8, from equine serum), 5,5'-dithiobis-(2-nitrobenzoic acid) (Ellman's reagent, DTNB), S-butrylthiocholine iodide (BTCl), acetylthiocholine iodide (ATCl), and larchine hydrochloride were purchased from Sigma–Aldrich. The capacity of the test compounds (**3a** and **13a–u**) to inhibit AChE and BuChE activities was assessed by Ellman's method. Stock solution of test compounds was dissolved in a minimum volume of DMSO (1%) and was diluted using the buffer solution (50 mM Tris–HCl, pH = 8.0, 0.1 M NaCl, 0.02 M $\text{MgCl}_2 \cdot 6\text{H}_2\text{O}$). In 96-well plates, 160 μL of 1.5 mM DTNB, 50 μL of AChE (0.22 U/mL prepared in 50 mM Tris–HCl, pH = 8.0, 0.1% w/v bovine serum albumin, BSA) or 50 μL of BuChE (0.12 U/mL prepared in 50 mM Tris–HCl, pH = 8.0, 0.1% w/v BSA) were incubated with 10 μL of various concentrations of test compounds (0.001–100 μM) at 37 °C for 6 min followed by the addition of the substrates (30 μL) acetylthiocholine iodide (15 mM) or S-butrylthiocholine iodide (15 mM) and the absorbance was measured at different time intervals (0, 60, 120, and 180 s) at a wavelength of 405 nm. The concentration of compound producing 50% of enzyme activity inhibition (IC_{50}) was calculated by nonlinear regression analysis of the response–concentration (log) curve, using the Graph-Pad Prism program package (GraphPad Software; San Diego, CA). Results are expressed as the mean \pm SEM of at least three different experiments performed in triplicate.

4.3. Kinetic analysis of ChE inhibition

To obtain of the mechanism of action **13s**, reciprocal plots of 1/velocity versus 1/[substrate] were constructed at different concentrations of the substrate thiocholine iodide (0.05–0.5 mM) by

using Ellman's method [48]. Three concentrations of **13s** were selected for the studies: 30.8, 15.4 and 7.7 nM for the kinetic analysis of AChE inhibition, and 90.0, 45.0, 22.5 nM for the kinetic analysis of BuChE inhibition, respectively. The plots were assessed by a weighted least-squares analysis that assumed the variance of velocity (v) to be a constant percentage of v for the entire data set. Slopes of these reciprocal plots were then plotted against the concentration of **13s** in a weighted analysis and K_i was determined as the intercept on the negative x-axis. Data analysis was performed with GraphPad Prism 4.03 software (GraphPad Software Inc.).

4.4. Molecular modeling studies

Molecular modeling calculations and docking studies were performed using Molecular Operating Environment (MOE) software version 2008.10 (Chemical Computing Group, Montreal, Canada). The X-ray crystallographic structure of AChE complexed with bis(7)–tacrine (PDB code 2CKM) was obtained from the Protein Data Bank. All water molecules in PDB files were removed and hydrogen atoms were subsequently added to the protein. The compound **13s** was built using the builder interface of the MOE program and energy minimized using MMFF94x force field. Then the **13s** was docked into the active site of the protein by the “Triangle Matcher” method, which generated poses by aligning the ligand triplet of atoms with the triplet of alpha spheres in cavities of tight atomic packing. The Dock scoring in MOE software was done using ASE scoring function and Forcefield was selected as the refinement method. The best 10 poses of molecules were retained and scored. After docking, the geometry of resulting complex was studied using the MOE's pose viewer utility.

4.5. Inhibition of A β (1–42) self-induced aggregation

Inhibition of A β (1–42) aggregation was measured using a Thioflavin T (ThT)-binding assay previously described by Bartolini et al. [49,50] with little modifications. A β (1–42) was dissolved in 100% 1,1,1,3,3,3-hexafluoro-2-propanol (HFIP) to a concentration of 1 mg/mL, sonicated in a water bath for 10 min, aliquoted into micro-centrifuge tubes, dried under vacuum, and stored in –20 °C. For the inhibition of self-induced A β (1–42) aggregation experiment, the A β was diluted with 50 mM phosphate buffer (pH 7.4) to 50 μM before use. A mixture of the peptide (10 μL , 25 μM , final concentration) with or without the tested compounds (10 μL) at different concentrations (2.5, 5, 10, 20, 40 μM) were incubated at 37 °C for 48 h. Blanks using 50 mM phosphate buffer (pH 7.4) instead of A β with or without inhibitors were also carried out. After incubation, the samples were diluted to a final volume of 200 μL with 50 mM glycine–NaOH buffer (pH 8.0) containing thioflavin T (5 μM). Then the fluorescence intensities were measured on a SpectraMax M5 (Molecular Devices, Sunnyvale, CA, USA) multi-mode plate reader with excitation and emission wavelengths at 446 nm and 490 nm, respectively. Each inhibitor was examined in triplicate. The fluorescence intensities were compared and the percent inhibition due to the presence of the inhibitor was calculated by the following formula: $(1 - \text{IF}_i/\text{IF}_0) \times 100\%$ where IF_i and IF_0 are the fluorescence intensities obtained for A β (1–42) in the presence and in the absence of inhibitors after subtracting the background, respectively.

4.6. Spectrophotometric measurement of complex with Cu^{2+} and Fe^{2+}

The study of metal chelation was performed in methanol at 298 K using UV–vis spectrophotometer (SHIMADZU UV-2450PC) with wavelength ranging from 200 to 500 nm [51,52]. The

difference UV–vis spectra due to complex formation was obtained by numerical subtraction of the spectra of the metal alone and the compound alone (at the same concentration used in the mixture) from the spectra of the mixture. A fixed amount of **13k** (25 $\mu\text{mol/L}$) was mixed with growing amounts of copper ion (2–50 $\mu\text{mol/L}$) and tested the difference UV–vis spectra to investigate the ratio of ligand/metal in the complex.

4.7. SH-SY5Y neuroblastoma cell toxicity

The toxicity effect of **13k** on the human neuroblastoma cell line SH-SY5Y cells was examined according to the previous methods [33,53]. The SH-SY5Y cells were cultured in Eagle's minimum essential medium (EMEM)/ham's F-12 (1:1) medium supplemented with 10% fetal bovine serum (FBS), 100 U/mL penicillin and 100 $\mu\text{g/mL}$ streptomycin, at 37 °C in a humidified atmosphere containing 5% CO₂.

Cells were subcultured in 96-well plates at a seeding density of 10,000 cells per well and allowed to adhere and grow. When cells reached the required confluence, they were placed into serum-free medium and treated with compound **13k**. Twenty-four hours later the survival of cells was determined by MTT assay. Briefly, after incubation with 20 μL of MTT at 37 °C for 4 h, living cells containing MTT formazan crystals were solubilized in 200 μL DMSO. The absorbance of each well was measured using a microculture plate reader with a test wavelength of 570 nm and a reference wavelength of 630 nm. Results are expressed as the mean \pm SD of three independent experiments.

4.8. Hepatotoxicity studies [7]

The experiments were carried out on adult male ICR mice (weighing 18–22 g), which were purchased from Comparative Medicine Centre, Yangzhou University. Tacrine hydrochloride hydrate was dissolved in CMC-Na solution (0.5 g CMC-Na in 100 mL of distilled water) and 3 mg/100 g b wt, corresponding to 11.86 $\mu\text{mol}/100$ g b wt, were given in id. Test compounds were dissolved in CMC-Na solution, and the equimolar dose corresponding to tacrine was administered id. Heparinized serum was obtained 8, 20, and 30 h after dosing from the retrobulbar plexus to determine aspartate aminotransferase (ASAT) and alanine aminotransferase (ALT) activity, two indicators of a liver damage, using routine methods.

Acknowledgments

This research work was financially supported by Innovative Research Team in University (IRT1193), A Project Funded by the Priority Academic Program Development of Jiangsu Higher Education Institutions (PAPD), Project of Graduate Education Innovation of Jiangsu Province (No. CXZZ13_0320).

Appendix A. Supplementary data

These data include MOL files and InChIKeys of the most important compounds described in this article. Supplementary data associated with this article can be found in the online version, at <http://dx.doi.org/10.1016/j.ejmech.2013.09.024>. These data include MOL files and InChIKeys of the most important compounds described in this article.

References

- [1] E. Scarpini, P. Scheltens, H. Feldman, *Lancet Neurol.* 2 (2003) 539–547.
- [2] L. Piazzini, A. Rampa, A. Bisi, S. Gobbi, F. Belluti, A. Cavalli, M. Bartolini, V. Andrisano, P. Valenti, M. Recanatini, *J. Med. Chem.* 46 (2003) 2279–2282.
- [3] V. Tumiatti, A. Minarini, M.L. Bolognesi, A. Milelli, M. Rosini, C. Melchiorre, *Curr. Med. Chem.* 17 (2010) 1825–1838.
- [4] H.W. Querfurth, F.M. LaFerla, *N. Engl. J. Med.* 362 (2010) 329–344.
- [5] Q. Xie, H. Wang, Z. Xia, M. Lu, W. Zhang, X. Wang, W. Fu, Y. Tang, W. Sheng, W. Li, W. Zhou, X. Zhu, Z. Qiu, H. Chen, *J. Med. Chem.* 51 (2008) 2027–2036.
- [6] R.T. Bartus, R.L. Dean, B. Beer, A.S. Lipka, *Science* 217 (1982) 408–417.
- [7] Y. Chen, J. Sun, L. Fang, M. Liu, S. Peng, H. Liao, J. Lehmann, Y. Zhang, *J. Med. Chem.* 55 (2012) 4309–4321.
- [8] M. Harel, L.K. Sonoda, I. Silman, J.L. Sussman, T.L. Rosenberry, *J. Am. Chem. Soc.* 130 (2008) 7856–7861.
- [9] S. Butini, G. Campiani, M. Borriello, S. Gemma, A. Panico, M. Persico, B. Catalanotti, S. Ros, M. Brindisi, M. Agnusdei, I. Fiorini, V. Nacci, E. Novellino, T. Belinskaya, A. Saxena, C. Fattorusso, *J. Med. Chem.* 51 (2008) 3154–3170.
- [10] Y. Bourne, P. Taylor, Z. Radic, P. Marchot, *EMBO J.* 22 (2003) 1–12.
- [11] A.E. Reyes, M.A. Chacon, M.C. Dinamarca, W. Cerpa, C. Morgan, N.C. Inestrosa, *Am. J. Pathol.* 164 (2004) 2163–2174.
- [12] E. Ozturan Ozer, O.U. Tan, K. Ozadali, T. Kucukkilinc, A. Balkan, G. Ucar, *Bioorg. Med. Chem. Lett.* 23 (2013) 440–443.
- [13] G.V. De Ferrari, M.A. Canales, I. Shin, L.M. Weiner, I. Silman, N.C. Inestrosa, *Biochemistry* 40 (2001) 10447–10457.
- [14] P. Munoz-Ruiz, L. Rubio, E. Garcia-Palomo, I. Dorronsoro, M. del Monte-Millan, R. Valenzuela, P. Usan, C. de Austria, M. Bartolini, V. Andrisano, A. Bidon-Chanal, M. Orozco, F.J. Luque, M. Medina, A. Martinez, *J. Med. Chem.* 48 (2005) 7223–7233.
- [15] C. Chianella, D. Gragnaniello, P. Maisano Delsler, M.F. Visentini, E. Sette, M.R. Tola, G. Barbujani, S. Fuselli, *Eur. J. Clin. Pharmacol.* 67 (2011) 1147–1157.
- [16] J. Hardy, D.J. Selkoe, *Science* 297 (2002) 353–356.
- [17] I. Peretto, S. Radaelli, C. Parini, M. Zandi, L.F. Raveglia, G. Dondio, L. Fontanella, P. Misiano, C. Bigogno, A. Rizzi, B. Riccardi, M. Biscaioi, S. Marchetti, P. Puccini, S. Catinella, I. Rondelli, V. Cenacchi, P.T. Bolzoni, P. Caruso, G. Villetti, F. Facchinetti, E. Del Giudice, N. Moretto, B.P. Imbimbo, *J. Med. Chem.* 48 (2005) 5705–5720.
- [18] F. Belluti, M. Bartolini, G. Bottegoni, A. Bisi, A. Cavalli, V. Andrisano, A. Rampa, *Eur. J. Med. Chem.* 46 (2011) 1682–1693.
- [19] G. Liu, W. Huang, R.D. Moir, C.R. Vanderburg, B. Lai, Z. Peng, R.E. Tanzi, J.T. Rogers, X. Huang, *J. Struct. Biol.* 155 (2006) 45–51.
- [20] P. Zatta, D. Drago, S. Bolognin, S.L. Sensi, *Trends Pharmacol. Sci.* 30 (2009) 346–355.
- [21] C. Opazo, X. Huang, R.A. Cherny, R.D. Moir, A.E. Roher, A.R. White, R. Cappai, C.L. Masters, R.E. Tanzi, N.C. Inestrosa, A.I. Bush, *J. Biol. Chem.* 277 (2002) 40302–40308.
- [22] J. Dong, C.S. Atwood, V.E. Anderson, S.L. Siedlak, M.A. Smith, G. Perry, P.R. Carey, *Biochemistry* 42 (2003) 2768–2773.
- [23] X. Huang, R.D. Moir, R.E. Tanzi, A.I. Bush, J.T. Rogers, *Ann. N. Y. Acad. Sci.* 1012 (2004) 153–163.
- [24] M.L. Bolognesi, A. Cavalli, L. Valgimigli, M. Bartolini, M. Rosini, V. Andrisano, M. Recanatini, C. Melchiorre, *J. Med. Chem.* 50 (2007) 6446–6449.
- [25] V. Tumiatti, A. Milelli, A. Minarini, M. Rosini, M.L. Bolognesi, M. Micco, V. Andrisano, M. Bartolini, F. Mancini, M. Recanatini, A. Cavalli, C. Melchiorre, *J. Med. Chem.* 51 (2008) 7308–7312.
- [26] J. Hardy, *J. Neurochem.* 110 (2009) 1129–1134.
- [27] P.B. Watkins, H.J. Zimmerman, M.J. Knapp, S.I. Gracon, K.W. Lewis, *J. Am. Med. Assoc.* 271 (1994) 992–998.
- [28] S.I. Gracon, M.J. Knapp, W.G. Berghoff, M. Pierce, R. DeJong, S.J. Lobbstaal, J. Symons, S.L. Dombey, F.A. Luscombe, D. Kraemer, *Alzheimer Dis. Assoc. Disord.* 12 (1998) 93–101.
- [29] X. Chen, K. Zenger, A. Lupp, B. Kling, J. Heilmann, C. Fleck, B. Kraus, M. Decker, *J. Med. Chem.* 55 (2012) 5231–5242.
- [30] A. Musial, M. Bajda, B. Malawska, *Curr. Med. Chem.* 14 (2007) 2654–2679.
- [31] M.I. Rodriguez-Franco, M.I. Fernandez-Bachiller, C. Perez, B. Hernandez-Ledesma, B. Bartolome, *J. Med. Chem.* 49 (2006) 459–462.
- [32] M.I. Fernandez-Bachiller, C. Perez, L. Monjas, J. Rademann, M.I. Rodriguez-Franco, *J. Med. Chem.* 55 (2012) 1303–1317.
- [33] M.I. Fernandez-Bachiller, C. Perez, G.C. Gonzalez-Munoz, S. Conde, M.G. Lopez, M. Villarroya, A.G. Garcia, M.I. Rodriguez-Franco, *J. Med. Chem.* 53 (2010) 4927–4937.
- [34] I. Uriarte-Pueyo, M.I. Calvo, *Curr. Med. Chem.* 18 (2011) 5289–5302.
- [35] M. Katalinic, G. Rusak, J. Domacovic Barovic, G. Sinko, D. Jelic, R. Antolovic, Z. Kovarik, *Eur. J. Med. Chem.* 45 (2010) 186–192.
- [36] H. Lou, P. Fan, R.G. Perez, *Bioorg. Med. Chem.* 19 (2011) 4021–4027.
- [37] H. Kim, B.S. Park, K.G. Lee, C.Y. Choi, S.S. Jang, Y.H. Kim, S.E. Lee, *J. Agric. Food Chem.* 53 (2005) 8537–8541.
- [38] X. He, H.M. Park, S.J. Hyung, A.S. DeToma, C. Kim, B.T. Ruotolo, M.H. Lim, *Dalton. Trans.* 41 (2012) 6558–6566.
- [39] S.S. Xie, X.B. Wang, J.Y. Li, L. Yang, L.Y. Kong, *Eur. J. Med. Chem.* 64 (2013) 540–553.
- [40] M.L. Bolognesi, V. Andrisano, M. Bartolini, R. Banzi, C. Melchiorre, *J. Med. Chem.* 48 (2005) 24–27.
- [41] S.D. Taverna, H. Li, A.J. Ruthenburg, C.D. Allis, D.J. Patel, *Nat. Struct. Mol. Biol.* 14 (2007) 1025–1040.
- [42] L. Costantino, G. Rastelli, A. Albasini, *Eur. J. Med. Chem.* 31 (1996) 693–699.
- [43] M. Ono, N. Yoshida, K. Ishibashi, M. Haratake, Y. Arano, H. Mori, M. Nakayama, *J. Med. Chem.* 48 (2005) 7253–7260.
- [44] M. Ono, M.P. Kung, C. Hou, H.F. Kung, *Nucl. Med. Biol.* 29 (2002) 633–642.

- [45] S.Y. Zheng, Z.W. Shen, *Tetrahedron Lett.* 51 (2010) 2883–2887.
- [46] Y. Zhang, Z. Lv, H. Zhong, D. Geng, M. Zhang, T. Zhang, Y. Li, K. Li, *Eur. J. Med. Chem.* 53 (2012) 356–363.
- [47] P. Szymanski, A. Karpinski, E. Mikiciuk-Olasik, *Eur. J. Med. Chem.* 46 (2011) 3250–3257.
- [48] G.L. Ellman, K.D. Courtney, V. Andres Jr., R.M. Feather-Stone, *Biochem. Pharmacol.* 7 (1961) 88–95.
- [49] M. Bartolini, C. Bertucci, M.L. Bolognesi, A. Cavalli, C. Melchiorre, V. Andrisano, *Chembiochem* 8 (2007) 2152–2161.
- [50] S.Y. Chen, Y. Chen, Y.P. Li, S.H. Chen, J.H. Tan, T.M. Ou, L.Q. Gu, Z.S. Huang, *Bioorg. Med. Chem.* 19 (2011) 5596–5604.
- [51] R. Joseph, B. Ramanujam, A. Acharya, A. Khutia, C.P. Rao, *J. Org. Chem.* 73 (2008) 5745–5758.
- [52] W. Huang, D. Lv, H. Yu, R. Sheng, S.C. Kim, P. Wu, K. Luo, J. Li, Y. Hu, *Bioorg. Med. Chem.* 18 (2010) 5610–5615.
- [53] H. Zheng, M.B. Youdim, M. Fridkin, *J. Med. Chem.* 52 (2009) 4095–4098.
- [54] R.A. Osseni, C. Debbasch, M.O. Christen, P. Rat, J.M. Warnet, *Toxicol. In Vitro* 13 (1999) 683–688.